Remote Sensing of Environment xxx (xxxx) 113542

Contents lists available at ScienceDirect

Remote Sensing of Environment

journal homepage: www.elsevier.com/locate/rse

Fractional vegetation cover ratio estimated from radiative transfer modeling outperforms spectral indices to assess fire severity in several Mediterranean plant communities

José Manuel Fernández-Guisuraga [a, b, *], Leonor Calvo [b], Carmen Quintano [c, d], Alfonso Fernández-Manso [e], Paulo M. Fernandes [a]

[a] Centro de Investigação e de Tecnologias Agroambientais e Biológicas, Universidade de Trás-os-Montes e Alto Douro, 5000-801 Vila Real, Portugal
[b] Department of Biodiversity and Environmental Management, Faculty of Biological and Environmental Sciences, University of León, 24071 León, Spain
[c] Electronic Technology Department, School of Industrial Engineering, University of Valladolid, 47011 Valladolid, Spain
[d] Sustainable Forest Management Research Institute, University of Valladolid-Spanish National Institute for Agriculture and Food Research and Technology (INIA), 34004 Palencia, Spain
[e] Agrarian Science and Engineering Department, School of Agricultural and Forestry Engineering, University of León, 24400 Ponferrada, Spain

ARTICLE INFO

Edited by Dr. Marie Weiss

Keywords:
Composite Burn Index
dNBR
FCOVER
Mediterranean communities
PROSAIL-D
Transferability

ABSTRACT

The obtention of wall-to-wall fire severity estimates through reliable remote sensing-based techniques that align with management needs is a critical factor in post-fire decision-making processes. In this paper, we novelty proposed a multi-date change detection framework based on the variation in fractional vegetation cover (FCOVER), with enough ecological sense and physical basis to be generalizable across different plant communities and burned landscapes with varying environmental conditions. This framework meets the definition of fire severity operationally used in the field as a biophysical indicator when fire effects on the understory and overstory layers are linked. The FCOVER was retrieved from Sentinel-2 surface reflectance scenes by inverting PROSAIL-D radiative transfer model (RTM) simulations using the random forest regression algorithm. FCOVER retrievals were validated in the field using burned and unburned control plots. We computed the FCOVERr metric as the ratio of post-fire to pre-fire FCOVER. We tested the relationship of the FCOVERr and the most common bi-temporal spectral indices in the literature, i.e. the differenced Normalized Burn Ratio (dNBR), the Relative dNBR (RdNBR) and the Relativized Burn Ratio (RBR), with the Composite Burn Index (CBI) measured in field plots for validation purposes in two case-study wildfires in the western Mediterranean Basin. We also calculated the transferability of FCOVERr and the spectral indices between different plant communities within each site, as well as between sites. The predictive errors of pre and post-fire FCOVER retrievals were found to be low (RMSE ≈ 10%) for the two study sites. Overall, the FCOVERr metric provided more accurate CBI estimations (R^2 = 0.87 ± 0.04) than spectral indices (R^2 = 0.71 ± 0.13). The CBI was linearly related with the FCOVERr metric for both sites, whereas the type of relationship with spectral indices was not consistent, which translated into better transferability performance of the FCOVERr metric (nRMSE = 14.27% ± 3.75%) than that of the spectral indices (nRMSE = 21.97% ± 8.09%), not only between different Mediterranean plant communities within sites, but also between the two sites. Spectral indices underestimated moderate to high fire severity to a greater extent than FCOVERr in the CBI field plots, and misclassified fire severity in several areas with patchiness fire effects identified in the field. The FCOVERr product proposed in this study may be a sound choice for the operational identification of priority areas for post-fire management.

* Corresponding author at: Centro de Investigação e de Tecnologias Agroambientais e Biológicas, Universidade de Trás-os-Montes e Alto Douro, 5000-801 Vila Real, Portugal.
E-mail address: joseg@utad.pt (J.M. Fernández-Guisuraga).

https://doi.org/10.1016/j.rse.2023.113542
Received 17 November 2022; Received in revised form 1 March 2023; Accepted 8 March 2023
0034-4257/

1. Introduction

Wildfires are one of the most important disturbance factors in the terrestrial ecosystems of the Mediterranean Basin and in other Mediterranean-type areas of the world (Welch et al., 2016; Fernández-García et al., 2018). In the European Mediterranean region, wildfire disturbance affects about half a million forest hectares annually (San-Miguel-Ayanz et al., 2021), leading to massive atmosphere emissions in the form of greenhouse gases, black carbon and aerosols (Migliavacca et al., 2013), with important implications for land surface energy budgets (Ward et al., 2012) and thus for the climate system (Arneth et al., 2010; Archibald et al., 2018). At local scales, wildfires play an essential role shaping the species composition, structure and dynamics of Mediterranean plant communities (Díaz-Delgado et al., 2002; Tessler et al., 2016; Fernández-Guisuraga et al., 2019), as well as ecosystem functioning (Pérez-Valera et al., 2020; Sáenz de Miera et al., 2020), particularly under unprecedented fire disturbance regimes in the European Mediterranean Basin as a consequence of land use abandonment and extreme fire-weather (Fernandes et al., 2014; Nolè et al., 2022). Wildfires may also induce significant alterations in the soil properties (Certini, 2005), depending on the time-temperature history at the first centimeters of the soil (Santín and Doerr, 2016).

The magnitude of wildfire effects on the ecosystem can be measured in terms of fire severity (Lentile et al., 2006). This parameter is defined as the ecological changes on a burnt area regarding the pre-fire scenario (Key and Benson, 2005), and operationally measured as the above and belowground organic matter loss (Keeley, 2009). Although the terms fire severity and burn severity are used interchangeably, the former includes only short-term post-fire effects on the ecosystem (up to one year after fire), and the latter includes both short and long-term fire effects, including vegetation recovery responses (Lentile et al., 2006; Veraverbeke et al., 2010; Meng et al., 2017). In this study, the fire severity definition will be considered since the assessment of wildfire effects in the short term is essential for addressing on site stabilization/emergency actions (De Santis et al., 2009; Quintano et al., 2013) aimed at minimizing the most adverse ecological effects throughout the burned landscape. Previous research has established reliable methods for estimating fire severity in the field, based on the measurement of indicators such as percent change in canopy cover and basal area (Barden and Woods, 1976; Miller et al., 2009), height and depth of stem char (Hood et al., 2008), canopy scorch and consumption (Thompson and Spies, 2009), minimum tip diameter of remaining branches (Pérez and Moreno, 1998), forest-floor burn depth (Lewis et al., 2011), ash cover and depth (De Luis et al., 2003; Hudak et al., 2013), soil color and structure (Ketterings and Bingham, 2000; Vega et al., 2013) or soil chemical properties (Rodríguez-Alleres et al., 2012). Other common field-based assessments, such as the Composite Burn Index (CBI; Key and Benson, 2005), the Geometrically structured CBI (GeoCBI; De Santis and Chuvieco, 2009) and their predecessors (Ryan and Noste, 1983) and variants (Fernandes et al., 2010), are based on measuring several fire severity attributes using a multi-strata approach, rather than a single indicator. These indices score individual fire effects on four vegetation strata and substrate (i.e. two understory and three overstory strata), using a semiquantitative scale from unburned to completely or severely burned. The scores are linearly averaged by strata to produce a fire severity metric for the substrate, vegetation, and plot (considering all strata). The integrative nature of the (Geo)CBI is considered to provide an overall perspective of the fire impact on the ecosystem and improved feedback for land management (Fernández-García et al., 2018). Although the CBI was originally developed for calibrating Landsat bi-temporal spectral indices (Key and Benson, 2005), it has also been frequently used in studies based exclusively on field experimental designs (e.g. Kasischke et al., 2008). Nevertheless, methods based exclusively on field-based measurements are highly labor-intensive for assessing fire severity in large wildfires, do not allow wall-to-wall estimations, and often lack spatial thoroughness and representativeness (De Santis and Chuvieco, 2007).

Remote sensing has become an important data source for evaluating fire severity in extensive burned landscapes for its cost-effectiveness and synoptic nature (Yin et al., 2020a). Conventionally, spectral indices computed from passive optical data, such as the Normalized Burn Ratio (NBR; López-García and Caselles, 1991), the differenced NBR (dNBR; Key, 2006), the Relative dNBR (RdNBR; Miller et al., 2009) or the Relativized Burn Ratio (RBR; Parks et al., 2014), have been extensively used in recent years to estimate fire severity using empirical models in Mediterranean ecosystems (e.g. Norton et al., 2009; Harris et al., 2011; Fernández-García et al., 2018). However, spectral indices may show non-linear relationships with field severity indicators as a function of vegetation type, which hinders their transferability (Epting et al., 2005), they were initially designed to delimit burned areas, not to assess vegetation biophysical variability as a result of the fire (Roy et al., 2006; Lentile et al., 2009), and they do not use the full available optical spectrum in their formulation (De Santis et al., 2010). Strongly associated with the latter, spectral indices may not perform optimally at intermediate fire severity levels because a mixture of fire effects, characterized by complex spectral responses (Rogan and Franklin, 2001; Mallinis et al., 2018), is unlikely to be resolved in two discrete bands (Mitri and Gitas, 2008).

Physically-based methods applied to optical passive data, such as spectral unmixing models and radiative transfer models (RTMs), may be a sounder approach for estimating fire severity. Spectral unmixing models, including multiple endmember spectral mixture analysis (MESMA; Roberts et al., 1998), have been used to decompose reflectance signal of several ground components (i.e. endmembers) at sub-pixel level and estimate ground fraction images to be used as an input in fire severity classification (Meng et al., 2017). This approach is easily scalable, accounts for within-class spectral variability of the considered endmembers and the pixels can be modeled using different endmember combinations (Roberts et al., 1998). However, endmember collection is site-specific (Edwards et al., 2018) and capturing the inherent variability in the biophysical conditions of the species assemblage can be a challenging task in large burned landscapes (Fernández-Guisuraga et al., 2021a). In addition, multiple scattering elements in multi-layered or sparse canopies induces non-linear mixing that violates MESMA assumptions (Lentile et al., 2009). RTMs such as the coupled PROSPECT leaf model (Jacquemoud and Baret, 1990) and turbid-medium Kuusk canopy model (Kuusk, 2001) have been used to simulate the reflectance signal of fire effects in several forest strata (Chuvieco et al., 2006), being also inverted by De Santis and Chuvieco (2007) in a follow-up study to retrieve fire severity in terms of CBI from Landsat imagery. De Santis et al. (2009) and Yin et al. (2020a) inverted coupled PROSPECT and geometric canopy models, GeoSAIL (Huemmrich, 2001) and FRT (Kuusk and Nilson, 2000), respectively, which better represent the real conditions of forest canopy structure, for retrieving GeoCBI from Landsat and Sentinel-2 imagery. Despite the good performance and generalization ability of these models to simulate the post-fire spectral signatures of fire effects to retrieve the (Geo)CBI from optical data, their parameterization may be compromised immediately following the fire since they require knowledge of a large number of biophysical parameters per (Geo)CBI stratum from field data that sometimes are unavailable, particularly in the short-term after fire (Fernández-Guisuraga et al., 2021a).

In this paper, we aim to develop and validate a biophysical fire severity indicator, the variation in fractional vegetation cover (FCOVER), that can be used operationally because of its straightforward meaning and has enough ecological sense and physical basis to be generalized across Mediterranean plant communities. Specifically, we propose a bi-temporal or change detection framework, i.e. the post to pre-fire FCOVER ratio (FCOVERr), retrieved from passive optical data by inverting the PROSAIL-D RTM using a machine learning algorithm.

Here, we also propose an improvement of the FCOVER retrieval method (Fernández-Guisuraga et al., 2021b) by complementing PROSAIL-D simulations with representative endmember spectra of background materials in post-fire landscapes acquired from laboratory and field spectral libraries, as well as from an Airborne Visible/Infrared Imaging Spectrometer (AVIRIS) high spatial resolution image. This could expand the realism of the simulation scenarios to invert the RTM (Poulter et al., 2023), rather than the conventional endmember extraction from expected pure pixels of coarse satellite imagery (Verrelst et al., 2015), which can induce notable retrieval errors in heterogeneous burned landscapes (Fernández-Guisuraga et al., 2021b). FCOVER, defined as the vegetation fraction of a given ground extension (Gutman and Ignatov, 1998), is considered as an essential biophysical property in post-fire landscape assessments (Veraverbeke et al., 2012), and a reliable proxy for aboveground biomass and fuel loading in a wide variety of ecosystems worldwide (e.g. Flombaum and Sala, 2009; Jiang et al., 2017; Avitabile and Camia, 2018; Fernández-Guisuraga et al., 2021b). Although vegetation biophysical variables retrieved by the inversion of RTMs, such as the FCOVER, provide a direct link with field-based descriptors of fire severity because of the mechanistic relationship between the simulated reflectance by the models and the biophysical variation of the canopy as a consequence of the fire (Wang et al., 2022), these variables have not yet been applied to assess fire severity, particularly in bi-temporal or change detection frameworks. In this sense, FCOVER variation within a burned area meets the definition of fire severity to be used as a biophysical indicator (Verstraete and Pinty, 1996). Actually, the FCOVER retrieved from passive optical data quantifies the top-of-canopy vegetation fraction in single and multi-layered plant communities, also accounting in the latter case for the vegetation fraction sensed through canopy gaps (Fernández-Guisuraga et al., 2021a). However, we assume that understory and overstory fire effects in Mediterranean plant communities are correlated (Tanase et al., 2015). Under low-intensity surface fire scenarios, where such correlation is non-existent, the fire likewise does not have a major impact on the overall ecosystem function (Úbeda et al., 2006), and post-fire assessment is less critical (De Santis and Chuvieco, 2007). The opposite behavior, i.e. higher fire severities in the canopy than in the understory, is not realistic (Chuvieco et al., 2006). The FCOVERr product was validated in two case-study wildfires of the western Mediterranean Basin through a modified version of the CBI, considering the multi-strata fire severity attributes more related with the range of vegetation cover variation in the burned areas. We chose the CBI because it has been extensively and operationally used in fire severity assessments (e.g. in the Monitoring Trends in Burn Severity -MTBS- program; Picotte et al., 2020). In addition, it provides more reliable surrogates of post to pre-fire FCOVER variation through attributes such as the foliage consumption or percentage of green/black/brown foliage, than estimation using unburned nearby areas as pre-fire surrogates (Lentile et al., 2009). We expect that the FCOVERr metric will be more generalizable between the considered Mediterranean plant communities and burned landscapes than the most commonly used bi-temporal spectral indices (i.e. the dNBR, RdNBR and RBR) due to the physical basis of the RTM (De Santis and Chuvieco, 2007) and the ecological meaning of the variation in FCOVER (Roy et al., 2006).

2. Material and methods

2.1. Study sites and field-based fire severity measurements

Two case-study wildfires were selected in Spain (western Mediterranean Basin) based on the availability of field fire severity assessments and Sentinel-2 data: (i) Sierra de Cabrera site (Fig. 1A), in which 9940 ha of forest and shrubland burned in August 2017, and (ii) Navalacruz site (Fig. 1B), affected by a wildfire that burned 22,444 ha of forest, woodland and shrubland in August 2021. The study sites have

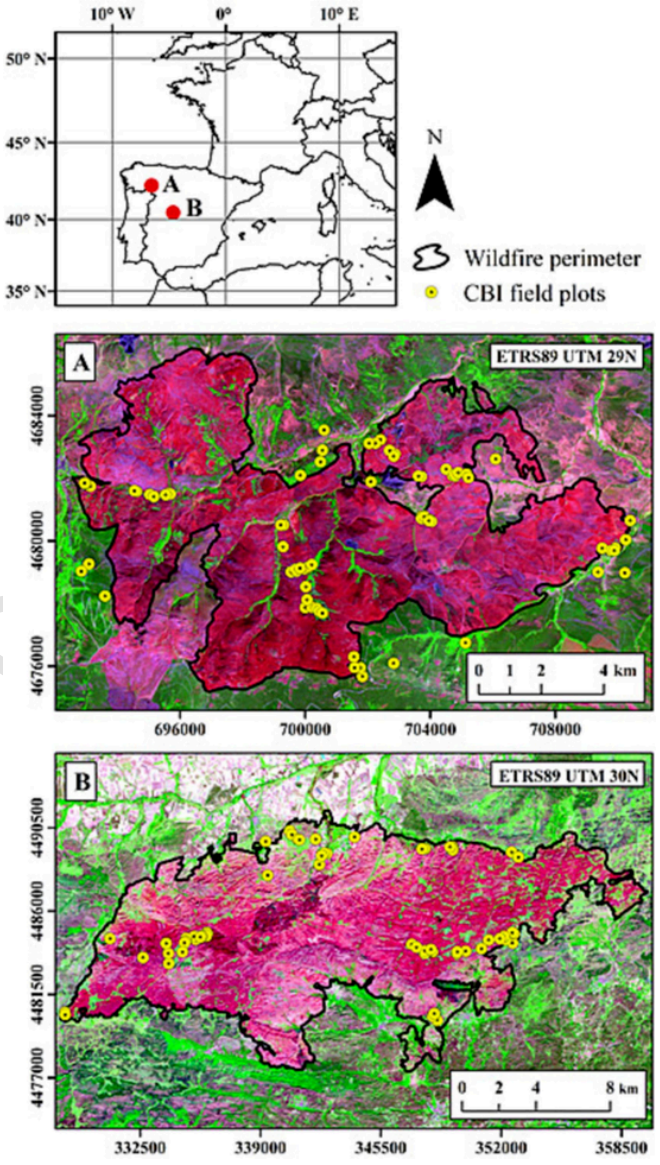

Fig. 1. Sierra de Cabrera (A) and Navalacruz (B) wildfires in Spain (western Mediterranean Basin), and location of the Composite Burn Index (CBI) field plots within the wildfires. The background image is a Sentinel-2 false color composite (R = band 12; G = band 8A; B = band 4).

rugged topography, with steep slopes, prominent crests and wide valleys, and altitudes ranging between 836 and 2157 m above sea level. The climate is classified as Mediterranean temperate, with a mean annual precipitation lower than 850 mm for a 50-year period (Ninyerola et al., 2005). Extreme weather conditions before the fire dates were recorded, i.e. a heat wave and severe drought episodes the weeks before the wildfires, which together with high wind speeds promoted extreme fire behavior.

In the Sierra de Cabrera site, the wildfire mainly affected forests dominated by *Quercus pyrenaica* Willd. (Pyrenean oak) and *Pinus sylvestris* L. (Scots pine), and shrublands dominated by *Genista hystrix* Lange (gorse) and *Erica australis* L. (Spanish heath). According to the Harmonized World Soil Database (Nachtergaele et al., 2010), soils in this site are classified as Lithic and Distric Leptosols, and Distric and Humic Cambisols (Fernández-Guisuraga et al., 2021b). The burned vegetation in the Navalacruz site comprised Scots pine forests, woodlands dominated by *Quercus ilex* L. (holm oak), and shrublands dominated by *Cytisus oromediterraneus* Rivas Mart. et al. (black broom). Soils are clas-

sified as Umbric Leptosols and Umbric Gleysols. The fire severity observed in the field was highly heterogeneous at both sites, with a marked patchy pattern probably arising from the variability in stand age, topography and local fire weather patterns.

Fire severity was assessed in the field within one month after each fire using a modified version (Table SM1 of the Supplementary Material) of the CBI defined by Key and Benson (2005) applied to plots of 20 m × 20 m georeferenced using a GPS receiver with sub-meter accuracy. We established 53 plots in Sierra de Cabrera and 63 plots in Navalacruz. We ensured a minimum distance of 100 m between plots. The plots were equally stratified within each site using the dominant plant communities as strata, both in burned and unburned control areas. We located the plots in homogeneous patches regarding vegetation structure and fire effects by visual inspection in the field to ensure a uniform spectral response (e.g. De Santis and Chuvieco, 2007; De Santis et al., 2009; Veraverbeke et al., 2010; Schepers et al., 2014; Fernández-Guisuraga et al., 2021a). In the understory layer, we recorded the fine fuel consumption for the substrate, and the percent foliage altered for the strata consisting of herbs, low shrubs and trees <1 m tall, as well as for the strata consisting of tall shrubs and trees between 1 and 5 m. In the overstory layer (i.e. intermediate trees with 5-20 m and trees taller than 20 m), we recorded the percentage of green/black/brown foliage. We did not consider ecosystem responses (e.g. new sprouts or seedlings) as an attribute because they were negligible (%cover $<0.1 \times 10^{-3}$) in the study sites one month after fire. The scores for the attributes in each stratum were obtained by the consensus of at least two observers (De Santis and Chuvieco, 2007). The plot-level CBI was then computed as the average of the attribute scores across all strata (where present). The remaining indicators of the original Key and Benson (2005) CBI protocol were also recorded in the field to compute the plot-level CBI from the original protocol and ensure that differences in the used CBI protocol are not responsible for the results of the FCOVERr metric and spectral indices comparison. The plot-level CBI did not significantly differ between the original and modified CBI protocols for both study sites (*p-values* > 0.27 of paired sample *t*-tests), being the score differences lower than 0.05 (CBI units) in all plots. This is expected since most of the CBI attributes per strata are ecologically correlated. Although the differences between the scores of the two protocols are minimal, the modified CBI protocol has more physical and ecological sense to be use in the validation of the FCOVERr metric. Also, the adaptation of field-based indicators to new remote sensing products is reasonable, since the CBI has been subject to frequent refinements that remain within the CBI conceptual framework (Lentile et al., 2006).

We considered the CBI thresholds proposed by Miller and Thode (2007): low (CBI < 1.25), moderate (1.25 ≤ CBI ≤ 2.25) and high (CBI > 2.25), which provided comparable fire effects in the plant communities at both study sites and were also used in modified CBI protocols (e.g. Fernández-Guisuraga et al., 2021a; Huerta et al., 2022). In low fire severity areas, the shrub foliage was partially consumed but the tree canopy was largely unaffected, whereas in the high fire severity areas, understory and overstory foliage consumption was nearly total. Moderate fire severity areas featured incomplete canopy foliage loss, but the degree of understory vegetation consumption was high.

2.2. Remote sensing data

Sentinel-2A Level 1C scenes for Sierra de Cabrera and Navalacruz sites were retrieved from the Open Access Hub of Copernicus in immediate pre and post-fire conditions for evaluating fire severity through the FCOVERr metric and bi-temporal spectral indices (Fig. 2). Scenes from one year after fire were also acquired to validate FCOVERr retrieval through contemporaneous field data. Acquisition dates were chosen based on the availability of cloud-free Sentinel-2 scenes as close as possible to the dates of interest (Table 1).

The ATCOR-3 algorithm (Richter and Schläpfer, 2018) was used to atmospherically and topographically correct Sentinel-2 scenes, obtaining a surface reflectance product (Level 2A). Ancillary data were used to set ATCOR-3 input parameters, including the MODIS water vapor product (MOD05), weather data from the State Meteorology Agency of Spain (AEMET) and the National Oceanic and Atmospheric Administration (NOAA), and a digital terrain model (DTM) at 5 m spatial resolution from the Spanish National Plan for Aerial Orthophotography (PNOA). The aerosol model type was set to rural and the visibility value was fixed to 40 km (clear weather conditions) for each Sentinel-2 scene. A mid-latitude summer MODTRAN model (water vapor content of 2.92 g cm^{-2}) was selected for scenes #1, #3, #4 and #6, and a sub-arctic summer MODTRAN model for scenes #2 and #5 (Table 1). Finally, the nearest neighbor interpolation algorithm was used to resample Sentinel-2 10 m bands to 20 m (Dörnhöfer et al., 2016; Fernández-Guisuraga et al., 2021b), whereas Sentinel-2 bands at 60 m spatial resolution were discarded from subsequent analyses since they are affected by atmospheric effects and are unable to deliver top-of-canopy reflectance interpretable by RTMs (Fernández-Guisuraga et al., 2021b).

2.3. FCOVER retrieval

A simulation dataset of matched FCOVER values and top-of-canopy reflectance was generated through the PROSPECT-D leaf model (Féret et al., 2017) and the 4SAIL canopy reflectance model (Verhoef et al., 2007), coupled in the PROSAIL-D RTM. PROSPECT-D was used to simulate leaf hemispherical transmittance and reflectance in the optical domain (400-2500 nm with a spectral resolution of 1 nm) using known ranges of several physiological and biochemical parameters at the leaf level in the plant communities (Féret et al., 2017): structure parameter (N), chlorophyll *a* and *b* (C_{a+b}), carotenoid (C_{car}), and anthocyanin (C_{ant}) concentration, brown pigments fraction (C_{brown}), dry matter content (C_m) and equivalent water thickness (C_w). The simulated leaf transmittance and reflectance served as input to the 4SAIL model, together with the following variables related to known canopy structure and viewing geometry conditions, to simulate turbid-medium, top-of-canopy spectral reflectance (Verhoef et al., 2007): leaf area index (LAI), average leaf angle (ALA), ratio between diffuse and direct radiation (diff/dir), hot spot effect (hspot), soil background reflectance, soil brightness factor (α_{soil}), and satellite viewing geometry conditions (solar zenith angle -θ_s-, observation zenith angle -θ_o- and sun-sensor azimuth angle -φ-). The fixed values or ranges of the RTM input variables (Table 2) were established on the basis of field knowledge regarding the biophysical conditions variability of the target plant communities in the study sites, the TRY database, literature review and satellite metadata (Baret et al., 2007; Kattge et al., 2011; Campos-Taberner et al., 2018; Fernández-Guisuraga et al., 2021a, 2021b, 2022a).

The entire PROSAIL-D variable space, defined by all the possible combinations of the model input variables, was sampled through the Latin Hypercube Sampling algorithm (McKay et al., 1979) to select 2000 reflectance simulations, which are typically enough to obtain reliable results in RTM approaches (Fernández-Guisuraga et al., 2021a). Following turbid-medium assumptions, FCOVER for each PROSAIL-D sample was computed from LAI, ALA and viewing geometry conditions using the classical gap fraction calculation (Jia et al., 2016). Then, PROSAIL-D samples were run in forward mode to obtain a simulation dataset of top-of-canopy reflectance values from 400 to 2500 nm with a spectral resolution of 1 nm and the corresponding FCOVER. PROSAIL-D execution in forward mode took less than two minutes to complete in an Intel Core i7 processor with 128Gb RAM. The dataset was expanded with 20% of soil, non-photosynthetic vegetation (NPV), char and ash representative spectra for our study sites. The ECOSTRESS (Meerdink et al., 2019) and European LUCAS Topsoil 2015 (Jones et al., 2020) laboratory spectral libraries were used as a resource of soil and NPV endmember spectra. Char and ash endmembers were collected from field-

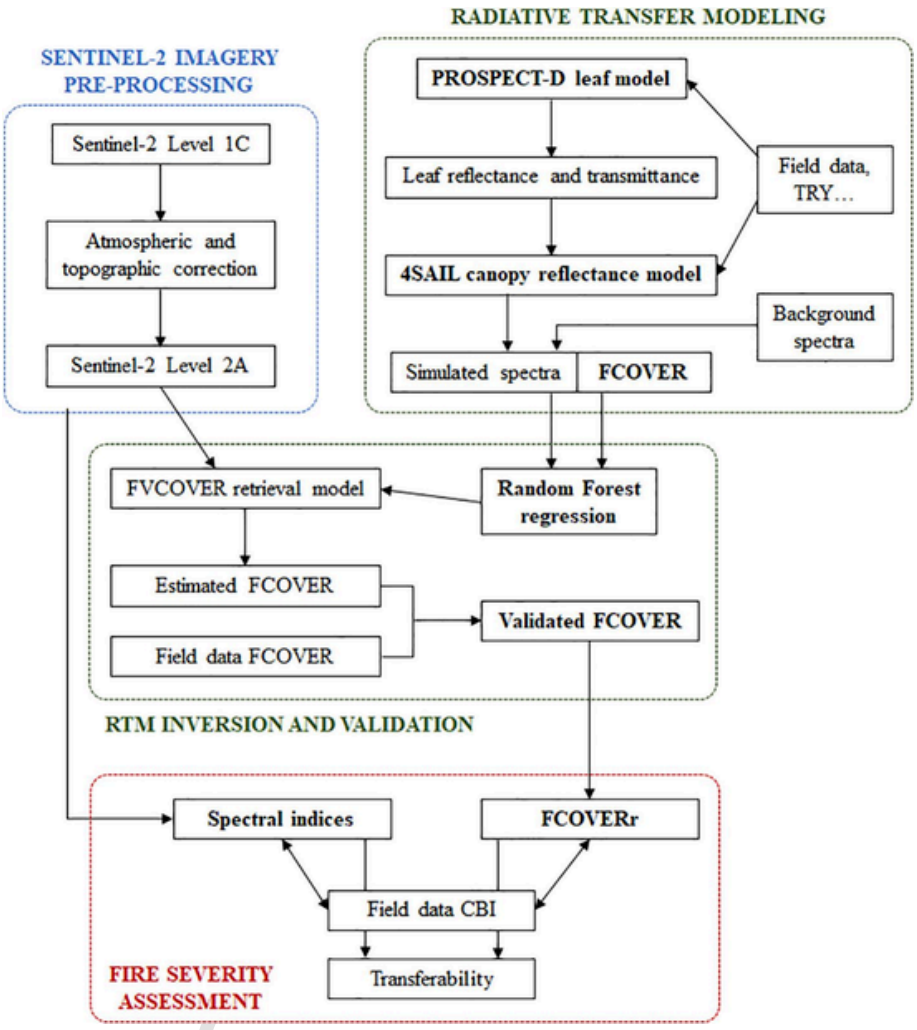

Fig. 2. Methodology flowchart of the present study.

Table 1
Acquisition dates of the Sentinel-2A Level 1C scenes.

Site	Scene #	Acquisition date	Date regarding fire
Sierra de Cabrera	1	13th August 2017	Immediately pre-fire
	2	2nd September 2017	Immediately post-fire
	3	14th July 2018	One year after fire
Navalacruz	4	9th August 2021	Immediately pre-fire
	5	8th October 2021	Immediately post-fire
	6	25th July 2022	One year after fire

based spectral libraries (Morgan et al., 2005), as well as from an Airborne Visible/Infrared Imaging Spectrometer (AVIRIS) image acquired at a spatial resolution of 7.5 m following a wildfire that burned several Mediterranean ecosystems of western United States in summer 2009 (Quintano et al., 2013). See Roberts et al. (2012) for details of the AVIRIS image processing. The performance of this approach (hereafter reference endmember) in the FCOVER retrieval was benchmarked with the original method developed by Fernández-Guisuraga et al. (2021b) that involves the complementation of PROSAIL-D simulations with endmember spectra acquired from expected pure pixels of the immediately post-fire Sentinel-2 image itself (hereafter image endmember). Endmember extraction from satellite images was based on image inspection and expert knowledge of the spectral signature shape of the candidate targets (Quintano et al., 2020). The updated reflectance datasets were resampled to match the band configuration of Sentinel-2 using its spectral bandwidth and relative spectral response. Gaussian noise of 2% was

Table 2
Fixed values or ranges of PROSPECT-D leaf model and 4SAIL canopy reflectance model.

Leaf RTM (PROSPECT-D)	Symbol	Unit	Fixed value or range
Structure parameter	N	unitless	1.5–2.5
Chlorophyll *a* and *b* concentration	C_{a+b}	μg cm^{-2}	10–90
Carotenoid concentration	C_{car}	μg cm^{-2}	5–40
Anthocyanin concentration	C_{ant}	μg cm^{-2}	0–50
Brown pigments fraction	C_{brown}	unitless	0–1
Dry matter content	C_m	g cm^{-2}	0.001–0.02
Equivalent water thickness	C_w	g cm^{-2}	0.001–0.02
Canopy RTM (4SAIL)	**Symbol**	**Unit**	**Fixed value or range**
Leaf area index	LAI	m^2 m^{-2}	0.1–6
Average leaf angle	ALA	°	20–90
Diffuse/direct radiation	diff/dir	unitless	0.1
Hot spot effect	hspot	unitless	0.001–1
Soil brightness factor	α_{soil}	unitless	0–1
Solar zenith angle	θ_s	°	Scene metadata
Observation zenith angle	θ_o	°	Scene metadata
Sun-sensor azimuth angle	φ	°	Scene metadata

added to the reflectance dataset to account for the uncertainty in the topographic and atmospheric corrections performed to satellite imagery (García-Haro et al., 2018).

The parameterization and execution of PROSAIL-D in forward mode were performed in Automated Radiative Transfer Models Operator (ARTMO) software (Verrelst et al., 2012).

The random forest regression (RFR; Breiman, 2001) algorithm was used to build the relationships between PROSAIL-D top-of-canopy reflectance simulations in the Sentinel-2 band configuration and the corresponding FCOVER for both study sites. The *ntree* RFR model parameter were set to 2000, which balances a stable out-of-bag error rate (Figure SM1 of the Supplementary Material) with computational efficiency (Probst and Boulesteix, 2018). The *mtry* parameter was tuned using 10-fold cross-validation (10-fold-CV) ten times repeated. The optimum mtry *value* according to the $RMSE_{10\text{-fold-CV}}$ was three, which matched the default value, i.e. one third of the number of Sentinel-2 bands (excluding the 60 m bands). These values maximized RFR model performance as measured by the out-of-bag error. The RFR model object was then applied to the actual surface reflectance of the Sentinel-2 Level 2A scenes (Table 1) for obtaining wall-to-wall FCOVER predictions for each pixel (i.e. FCOVER retrieval). The runtime of this procedure was about three minutes for each wildfire with the same computer setup than that used for PROSAIL-D execution in forward mode.

The FCOVER retrieval through the RFR algorithm was implemented in R 4.0.5 (R Core Team, 2021) using *RandomForest* (Liaw and Wiener, 2002), *raster* (Hijmans, 2021) and *rgdal* (Bivand et al., 2021) packages.

2.4. FCOVER retrieval validation

The FCOVER retrievals from Sentinel-2 imagery were validated using a set of field plots of 20 m × 20 m established one year after wildfire in Sierra de Cabrera (50 plots in burned areas and 10 plots in unburned control areas) and Navalacruz (65 plots in burned areas and 15 plots in unburned control areas) sites. A minimum distance of 100 m between plots was ensured. We assumed a similar FCOVER retrieval performance one year after fire as in the immediate post-fire situation. This is supported by the generalization ability of biophysical parameters' retrieval between different post-fire time scenarios in the same communities through adequately parametrized RTMs to reflect the biophysical settings of the target vegetation assemblages (Fernández-Guisuraga et al., 2021a), as in this study. Also, the unburned control approach supports the premise that the FCOVER retrieval from the pre-fire Sentinel-2 scenes would feature similar performance (Díaz-Delgado et al., 2002). The field plots were stratified into the dominant communities within each site, with the same number of plots for each community. By visual inspection in the field, the plots were located in homogeneous patches in terms of vegetation legacies in burned areas, and vegetation structure in control areas, to ensure a uniform spectral signal in the plots. The plots were geolocated similarly to the CBI plots. FCOVER was measured by at least two experienced observers as the vertical projection occupied by the existing vegetation strata using a visual estimation method at 5% intervals (Fernández-Guisuraga et al., 2022b) in four 2 m × 2 m subplots nested within 20 m × 20 m plots. The subplots were located 7 m away from the plot center at azimuths of 45°, 135°, 225° and 315°. In multi-layered communities, i.e. forest and woodland, a bottom-up FCOVER estimation was used for the overstory layer using a quadrat held by long sticks, whereas the FCOVER of the understory was estimated in a top-down direction through canopy gaps (Fernández-Guisuraga et al., 2021a). The FCOVER at the 20 m × 20 m plot level was obtained by averaging the FCOVER estimation in the four subplots. The performance of FCOVER retrievals for the two sites was evaluated through the coefficient of determination (R^2), the mean absolute error (MAE), the mean bias error (MBE) and the root mean squared error (RMSE) for the linear relationship between FCOVER measured in burned and in control field plots.

2.5. Remote sensing-based fire severity metrics and data analyses

The fire severity metric proposed in this paper, i.e. FCOVERr, is calculated as the ratio of post-fire to pre-fire FCOVER retrievals from Sentinel-2 scenes (Eq.1).

$$FCOVER_r = FCOVER_{post-fire} / FCOVER_{pre-fire} \quad (1)$$

The FCOVERr index ranges between 0 and 1. The higher the index value, the lower the FCOVER variation with respect to the pre-fire scenario and the lower the fire severity. The most commonly used bi-temporal spectral indices in the literature, i.e. the dNBR, RdNBR and RBR (Eq.5), were used as a benchmark method of the FCOVERr metric and calculated from Sentinel-2 surface reflectance bands according to Eq.2-Eq.5.

$$NBR_{Sentinel-2} = (Band\ 8A - Band\ 12) / (Band\ 8A + Band\ 12) \quad (2)$$

$$dNBR = 1000\left(NBR_{pre} - NBR_{post}\right) \quad (3)$$

$$RdNBR = dNBR / \left(\left|NBR_{pre-fire}\right|^{0.5}\right) \quad (4)$$

$$RBR = dNBR / \left(NBR_{pre} + 1.001\right) \quad (5)$$

The relationship between field estimates of fire severity (i.e. plot-level scores of the modified CBI protocol) and each remote sensing-based fire severity retrieval (i.e. FCOVERr metric and spectral indices) was evaluated through univariate ordinary least squares (OLS) models calibrated for each study site. We considered linear, quadratic and cubic predictor terms in the models to account for potential non-linear relationships, selecting the univariate model that featured the highest fit assessed by means of the R^2. The same analyses were conducted for the plot-level scores of the original CBI protocol to discard potential biases in the results.

The transferability of univariate OLS models (external model validation) was assessed between different plant communities within each site and between sites using data from all plant communities. For instance, the CBI-FCOVERr model output in one of the plant communities of Sierra de Cabrera site was applied to predict CBI in each of the other two plant communities of the site, iteratively. This process was repeated iteratively for all remote sensing-based fire severity retrievals between communities/sites. Model transferability performance was assessed using the normalized RMSE (nRMSE) from the maximum and minimum CBI observed value in the target community/site, with errors higher than 25% considered as unacceptable (De Santis and Chuvieco, 2007; Fernández-García et al., 2018).

The CBI thresholds suggested by Miller and Thode (2007) (section 2.1) and OLS model equations were used to define three fire severity categories (low, moderate and high) in the FCOVERr metric and in the spectral indices (i.e. thresholding approach) and generate wall-to-wall, categorized fire severity maps. These maps were qualitatively assessed through field observations, and quantitatively validated at landscape scale by means of high spatial resolution aerial/satellite remote sensing data following Quintano et al. (2013). Specifically, we used 2017 and 2020 pre-fire 25-cm resolution orthophotos provided by the PNOA as pre-fire reference data in Sierra de Cabrera and Navalacruz sites, respectively. Since post-fire orthophotos were not available for Navalacruz, we used immediately post-fire GEOSAT-2 (former Deimos-2) satellite pansharpened images to a spatial resolution of 75 cm for that purpose in both sites. We established a minimum of 50 sampling plots of 20 m × 20 m per fire severity class (low, moderate and high) and site following a random design. The plots were matched with the Sentinel-2 grid. A minimum separation of 100 m between CBI field plots and imagery reference plots was ensured. We assigned a fire severity class for each plot using a visual assessment of pre- and post-fire high spatial resolution imagery. We followed the criteria of Botella-Martínez and Fernández-Manso (2017). Low fire severity was assigned

to the plots in which the tree canopy remained mostly unaffected and the shrub areas were scorched. If more than half of the tree canopy layer was scorched and the shrub areas were mostly charred, the plots were classified as moderate severity. High-severity burned plots were characterized by almost total consumption of canopy and shrub foliage. We recognize that the photointerpretation process is subjective, but, following these criteria, fire severity classes assigned to the imagery reference plots were coherent with the categorized CBI scores of the field plots observed in the imagery. The classification performance of wall-to-wall, categorized fire severity maps (FCOVERr and spectral indices) was evaluated through the overall accuracy (OA) and the kappa index, as well as the producer's (PA) and user's (UA) accuracy for each fire severity class. We also computed patch description metrics at the class level to analyze the sensitivity of categorized fire severity maps in relation to the spatial patchiness of fire severity. We focused on two metrics that are commonly used in landscape assessments of burned areas (e.g. Farris et al., 2008; Nogueira et al., 2017; Skowronski et al., 2020): patch density (PD) and perimeter-area Fractal Dimension Index (p-a FDI) of each fire severity class. PD is an aggregation class metric that describes the fragmentation of each class in the landscape (McGarigal et al., 2012); p-a FDI describes the patch complexity of each class irrespective of scale, and high values correspond to more irregular shapes (McGarigal et al., 2012).

These metrics were computed in R 4.0.5 (R Core Team, 2021) using *raster* (Hijmans, 2021) and *landscapemetrics* (Hesselbarth et al., 2019) packages.

3. Results

The FCOVER retrieval from Sentinel-2 scenes one year after fire using reference endmembers to expand PROSAIL-D simulations with post-fire background spectra featured high overall fit and low predictive error for Sierra de Cabrera (R^2 = 0.80 and RMSE = 9.71%) and Navalacruz (R^2 = 0.86 and RMSE = 10.02%) sites in burned and control scenarios (Fig. 3). The retrievals were closely tailored to the 1:1 line, and only a slight underestimation was observed in the Sierra de Cabrera site throughout the whole FCOVER range (MBE = −4.61%). The retrieval performance was higher than that procured from PROSAIL-D simulations expanded with image endmembers (Figure SM2 of the Supplementary Material). The FCOVER estimated from the reference endmember approach was then considered for further analyses.

In the Sierra de Cabrera site, the mean FCOVER within the wildfire scar was equal to 53.79% ± 27.73% and 25.86% ± 10.61% in the immediate pre and post-fire situations, respectively (Fig. 4). The highest FCOVER values corresponded to valley-bottom areas dominated by Pyrenean oak forests burned at low and moderate fire severities. In Navalacruz site, the mean FCOVER in the immediate pre-fire conditions was equal to 45.60% ± 15.43% (Fig. 4), with the highest FCOVER observed in Scots pine forests and broom shrublands along a west-east axis in the central area of the wildfire scar. In post-fire conditions, with a mean FCOVER of 19.05% ± 11.77% (Fig. 4), the highest values were recorded in the north and south sections of the wildfire scar.

The relationship between the FCOVERr metric and the plot-level scores of the modified CBI protocol showed higher fit than the bi-temporal spectral indices in Sierra de Cabrera (R^2 = 0.89 vs R^2 = 0.76–0.84) and Navalacruz (R^2 = 0.84 vs R^2 = 0.50–0.68) through OLS models (Fig. 5). The best performing spectral indices were the dNBR and the RBR in both sites. The FCOVERr metric varied linearly with the CBI in both sites, whereas the type of relationship with spectral indices was not consistent between sites, even for the same spectral index (Fig. 5). For instance, dNBR and RBR indices featured a linear relationship with the CBI in Sierra de Cabrera site, but a quadratic relationship in Navalacruz site. The relationship between CBI and RdNBR was linear at both sites, but the RdNBR was the worst-performing index for retrieving fire severity. Similar results were evidenced for the plot-level scores of the original CBI protocol (Figure SM3 of the Supplementary Material).

As expected, this differential behavior translated into better transferability performance of the FCOVERr metric (nRMSE = 14.27% ± 3.75%) than for spectral indices (nRMSE = 21.97% ± 8.09%) between different plant communities within Sierra de Cabrera and Navalacruz sites, and also between the two sites (Fig. 6). Only for the model between Spanish heath shrublands (reference system) and Pyrenean oak forests (target system) transferability was higher using spectral indices (specifically dNBR) than using the FCOVERr metric (1 of 14 transferability cases analyzed). None of the transferability cases analyzed using the FCOVERr metric presented errors >25%, considered unacceptable, whereas five of the cases using spectral indexes did.

The wall-to-wall fire severity maps as estimated using the Miller and Thode (2007) CBI thresholds from the FCOVERr metric and the dNBR index fire severity retrievals are provided in Fig. 7. We chose the dNBR index because it showed the best performance in the field fire severity retrieval and is the most used operationally in programs such as the Monitoring Trends in Burn Severity (MTBS) project and the Rapid Damage Assessment (RDA) module of the European Forest Fire Information System (EFFIS). In the Sierra de Cabrera site, 41% of the surface was burned with high fire severity according to the FCOVERr metric, and 30% according to the dNBR. In contrast, fire severity retrieval using the

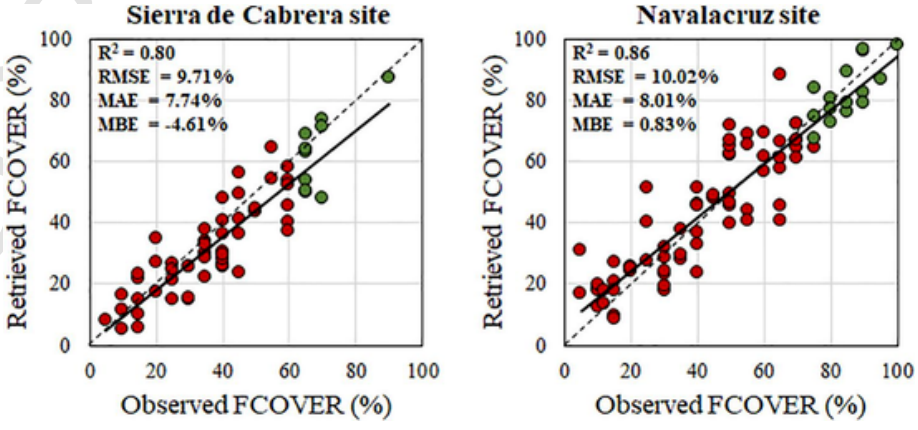

Fig. 3. Relationship between field-measured and retrieved FCOVER in burned (red) and control (green) plots one year after fire for Sierra de Cabrera and Navalacruz sites using reference endmembers to expand PROSAIL-D reflectance simulations with representative, post-fire background spectra. The dotted line represents the 1:1 line and the solid line the fit of the linear model. (For interpretation of the references to color in this figure legend, the reader is referred to the web version of this article.)

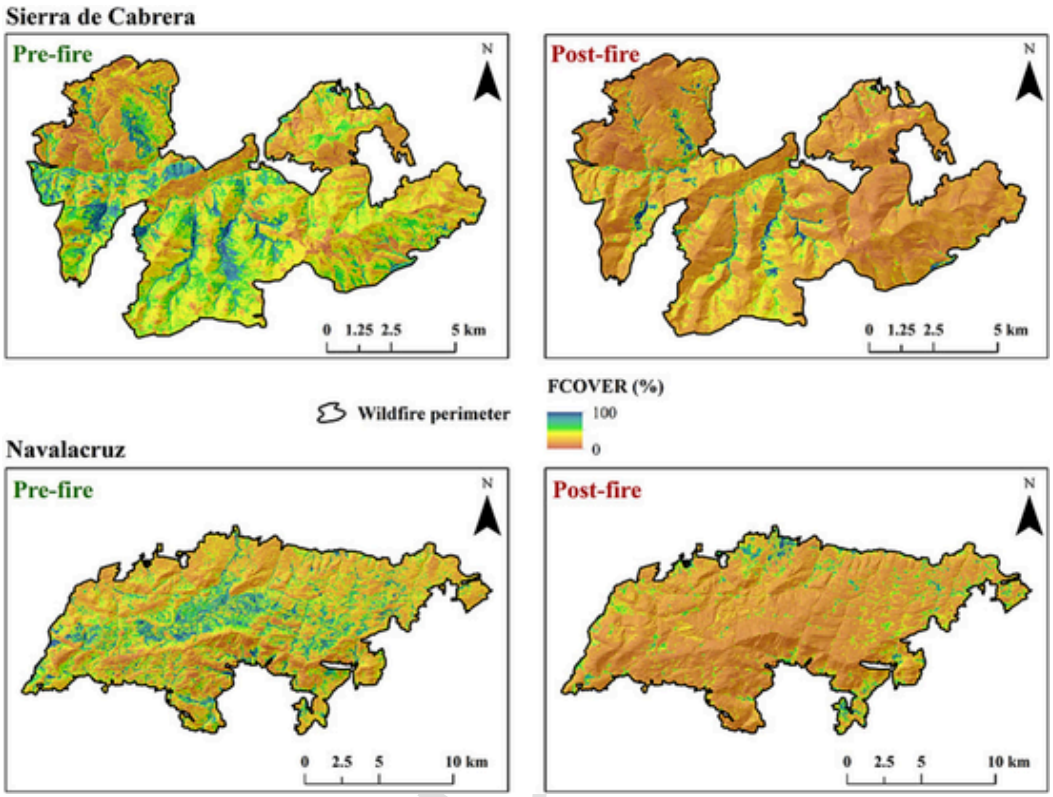

Fig. 4. Wall-to-wall FCOVER maps (20 m spatial resolution) in immediate pre and post-fire scenarios for Sierra de Cabrera and Navalacruz sites.

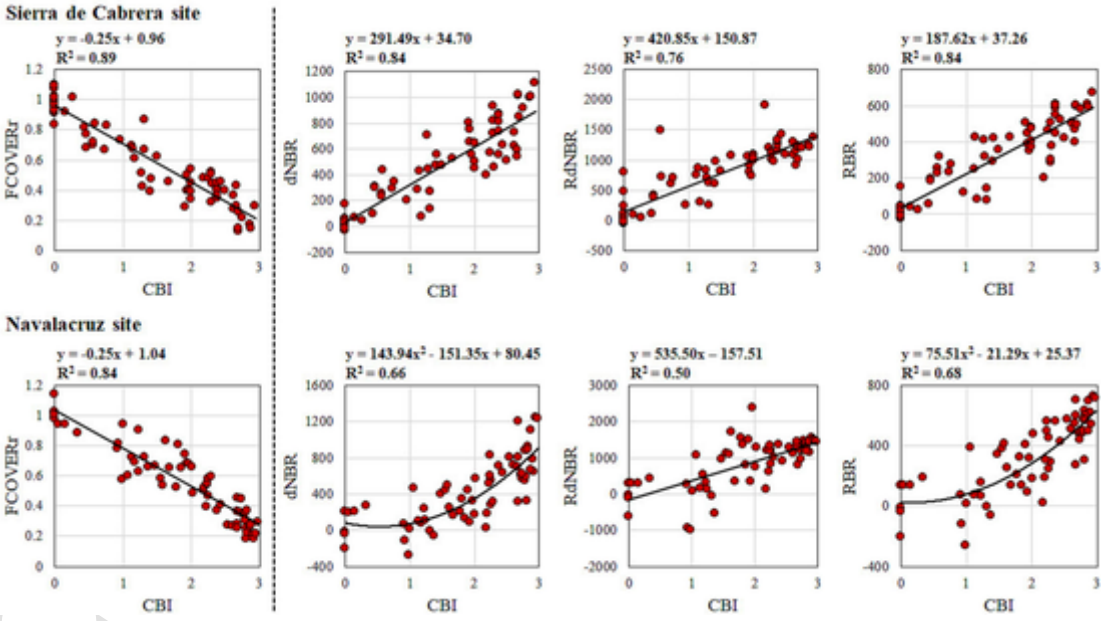

Fig. 5. Relationship between plot-level scores of the modified CBI protocol and remote sensing-based fire severity retrievals (i.e. FCOVERr metric and spectral indices) for Sierra de Cabrera and Navalacruz sites. The solid line represents the fit of the univariate ordinary least squares model evaluated through the coefficient of determination (R^2).

FCOVERr metric estimated a smaller burned area with high fire severity (30%) than the dNBR index (36%) in the Navalacruz site.

We found that the dNBR index did not adequately capture the spatial patterns of high vegetation damage in certain areas observed in the field and burned at high fire severity, for example some Scots pine stands in the Sierra de Cabrera site (Fig. 8A). This is consistent with the higher dNBR underestimation of moderate to high fire severity as compared to FCOVERr in the CBI field plots (Figure SM4 of the Supplementary Material). We also found by inspecting wall-to-wall maps and field observations that the FCOVERr metric captured better the variation in the spatial patchiness of low, moderate and high fire severity levels, especially in respect to narrow bands of moderate fire effects, for example in Pyrenean oak forests in Sierra de Cabrera (Fig. 8B). These observations were further confirmed by the quantitative assessment of catego-

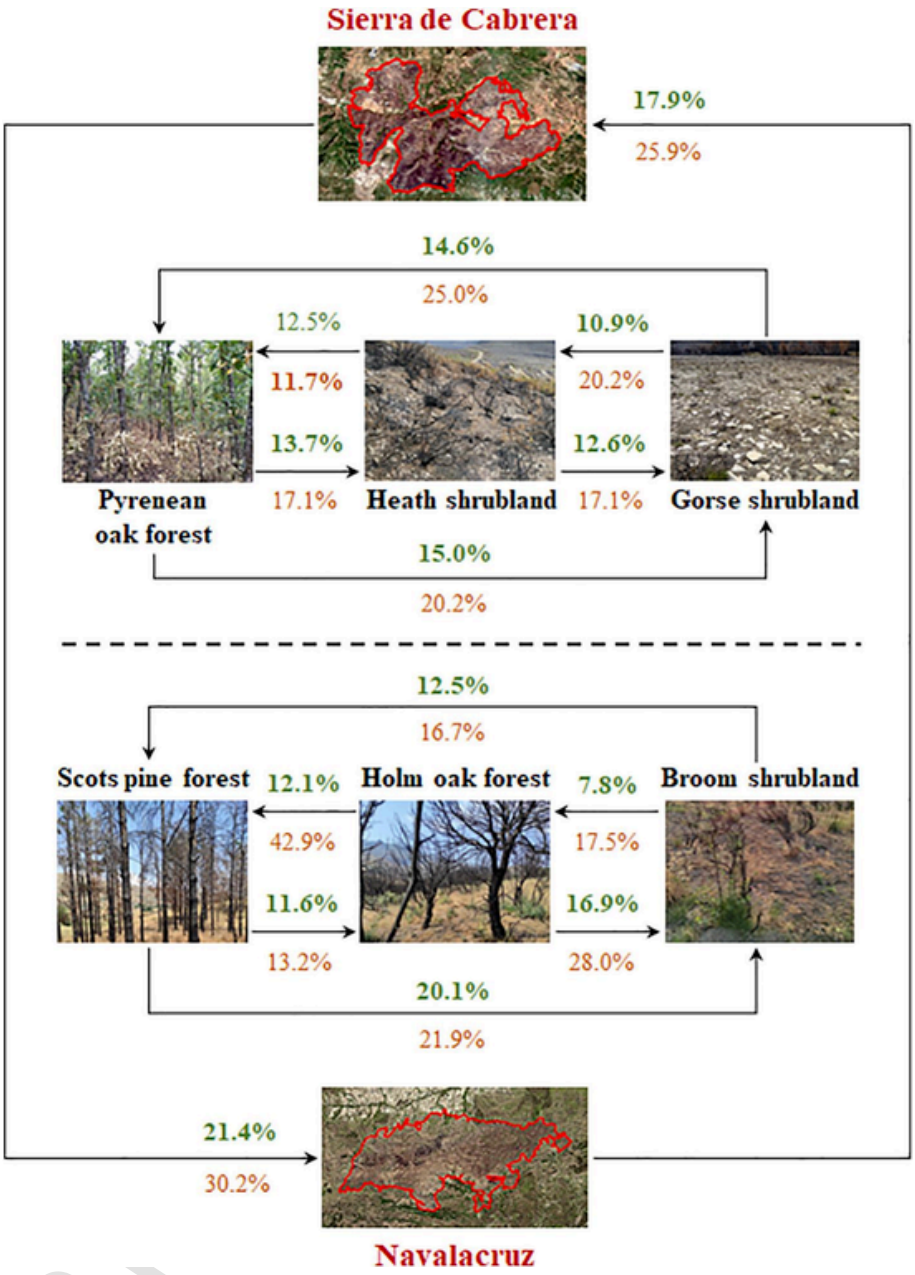

Fig. 6. Model transferability performance between different plant communities within Sierra de Cabrera and Navalacruz sites, and between the two sites, assessed through the normalized RMSE (nRMSE) from the maximum and minimum CBI observed value in the target community/site. The percentages in green represent the nRMSE corresponding to FCOVERr metric, and in red to the nRMSE of the best-performing spectral index in the transferability scheme. (For interpretation of the references to color in this figure legend, the reader is referred to the web version of this article.)

rized fire severity maps through fire severity reference data acquired from high spatial resolution aerial/satellite imagery, as well as by patch description metrics of each fire severity class. All classification accuracy metrics of FCOVERr were higher than those of the dNBR index, except for the PA of the low fire severity class in Navalacruz, which was higher for the dNBR index. The underestimation of high fire severity by the dNBR index was remarkable in both study sites, as well as the confusion of moderate fire severity class. Although present, both effects were less noticeable with the FCOVERr metric (Table 3). In addition, the density and shape complexity of patches for each fire severity class were higher in the FCOVERr maps than in dNBR maps, thus indicating that the capture of fire effects patchiness was improved (Table 4). This result is coherent with the relatively low misclassification of fire severity classes, particularly the moderate class, in the FCOVERr maps. For both fire severity metrics, patch density decreased in the high fire severity class (Table 4).

4. Discussion

Fire severity assessment through remote sensing-based techniques is not only a critical factor in post-fire management strategies (Morgan et al., 2014; Fernández-García et al., 2018) through wall-to-wall estimates that align with management needs (Keeley, 2009), but also has substantial implications for understanding the feedbacks of post-fire vegetation recovery dynamics (Meng et al., 2018; Yin et al., 2020a; Fernández-Guisuraga et al., 2021a). Indeed, satellite optical data have become a widely-used tool to assist in the identification of ecological changes induced by wildfires (Miller et al., 2009). The multi-date change detection framework novelty proposed in this study, i.e. the post to pre-fire

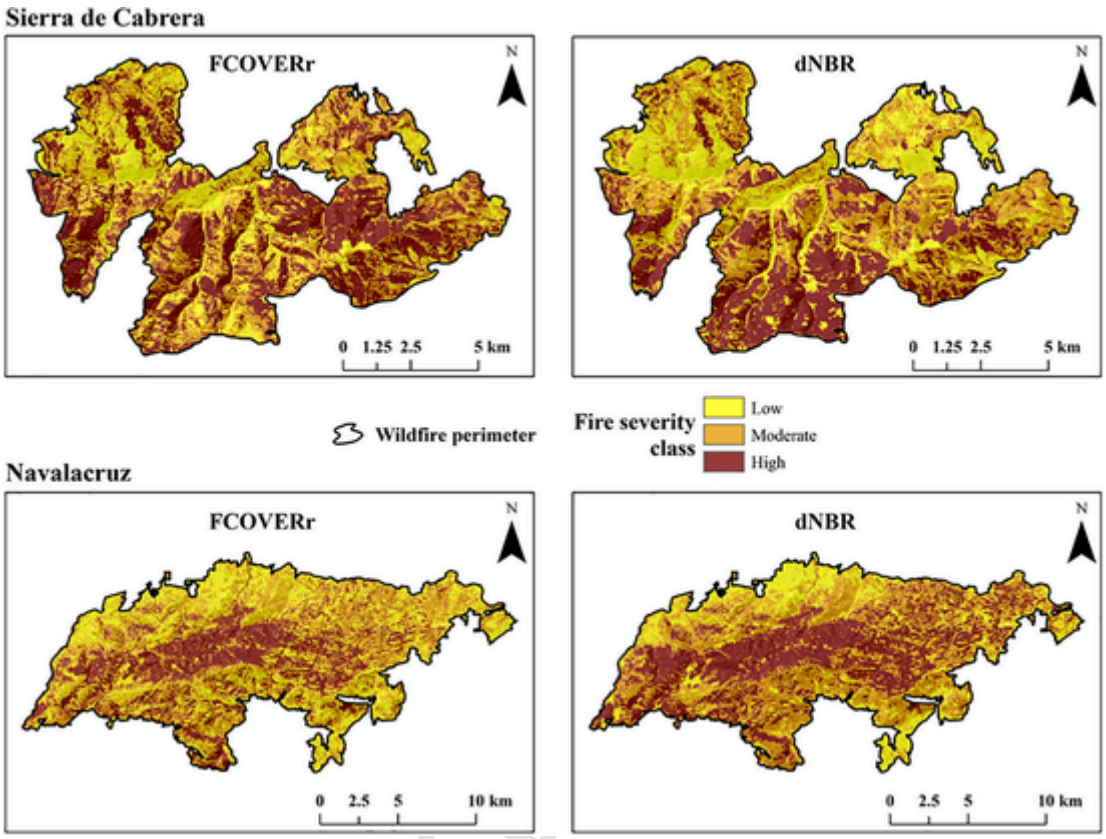

Fig. 7. Fire severity maps as estimated using the Miller and Thode (2007) CBI thresholds from the FCOVERr metric and the dNBR index fire severity retrievals.

FCOVER ratio retrieved from passive optical data by inverting the PROSAIL-D RTM, can be a sound choice as an operational metric for mapping fire severity from a remote sensing-based approach.

Previous remote sensing studies demonstrated that FCOVER is an essential biophysical property in the assessment of post-fire landscapes for its connections with the driving processes of the response of plant communities to fire disturbance (Fernández-Guisuraga et al., 2021a; Fernández-Guisuraga et al., 2022a). In this paper, we evidenced that the FCOVERr metric, estimated from a relative change perspective and considering the range of biophysical variation of heterogeneous vegetation communities within a burned landscape (Lentile et al., 2009), was consistent as a remote sensing descriptor of fire severity from an ecological standpoint (Miller and Thode, 2007) to be used as a biophysical indicator of fire damage. The basis of the proposed change detection approach in heterogeneous burned landscapes relied on the accurate characterization of FCOVER variability from optical data in burned and unburned scenarios. The inversion of the PROSAIL-D RTM featured accurate FCOVER estimates (RMSE ≤10%) in Mediterranean burned landscapes of the Iberian Peninsula, considered as a performance standard to be used as an operational product by end-users (Verrelst et al., 2016). The improvement of the FCOVER retrieval method introduced here, related to the expansion of PROSAIL-D reflectance simulations with post-fire background spectra from reference endmembers, may have led to a better spectral diversity characterization of the burned landscape (Hauser et al., 2021; Poulter et al., 2023) and thus to the observed performance increment with regard to the extraction of image endmembers for regulating the inversion scheme (Verrelst et al., 2015; Fernández-Guisuraga et al., 2021b). The FCOVER retrieval performance from satellite optical data at moderate spatial resolution using turbid-medium RTMs was consistent with previous research worldwide (Jia et al., 2016; Wang et al., 2018; Fernández-Guisuraga et al., 2021a). First, the physical basis inherent to RTMs allows high generalization ability in the retrieval scheme (De Santis et al., 2010), which can be exploited to estimate vegetation biophysical variability in heterogeneous landscapes comprising multiple vegetation communities with distinct species assemblages, as in our case-study sites (Fernández-Guisuraga et al., 2021b). Second, we simulated the relationship between canopy reflectance and FCOVER using the full available spectra in the optical images, contrary to local calibration using empirical models based on in situ data and spectral indices (Yin et al., 2020a). Third, the observed variability in the physiological and biochemical traits of the species assemblage in the plant communities at both sites may be translated into inconsistent reflectance spectra, even within a specific community (Asner, 1998). In this sense, PROSAIL-D RTM parametrization from a priori knowledge of the ranges of the model input variables for the plant communities of the sites would have adequately encompassed the vegetation biophysical variability in the reflectance simulation dataset (Fernández-Guisuraga et al., 2021a). And fourth, the PROSPECT-D leaf model within PROSAIL-D simulates leaf reflectance and transmittance incorporating the contribution of brown pigments and anthocyanins (Féret et al., 2017), which play an essential role in the vegetation leaf optical signal in post-fire plant communities under environmental stress and senescence conditions (Jacquemoud and Baret, 1990; Gould, 2004), particularly in the visible region of the spectrum (Yin et al., 2020b). Indeed, we determined through internal testing (not shown) that the consideration of brown pigments and anthocyanins in the retrieval scheme improved the FCOVER estimation under these conditions. The slight FCOVER underestimation evidenced in Sierra de Cabrera site may be attributed to a land cover aggregation effect of mixed pixels at the spatial resolution of Sentinel-2 (Fernández-Guisuraga et al., 2020) and the high ground spatial heterogeneity at this site (Fernández-Guisuraga et al., 2021b).

Overall, our results evidenced that the FCOVERr metric provided not only more accurate field fire severity retrievals than bi-temporal spectral indices in several Mediterranean plant communities of the case study sites, but also was more transferable between these plant commu-

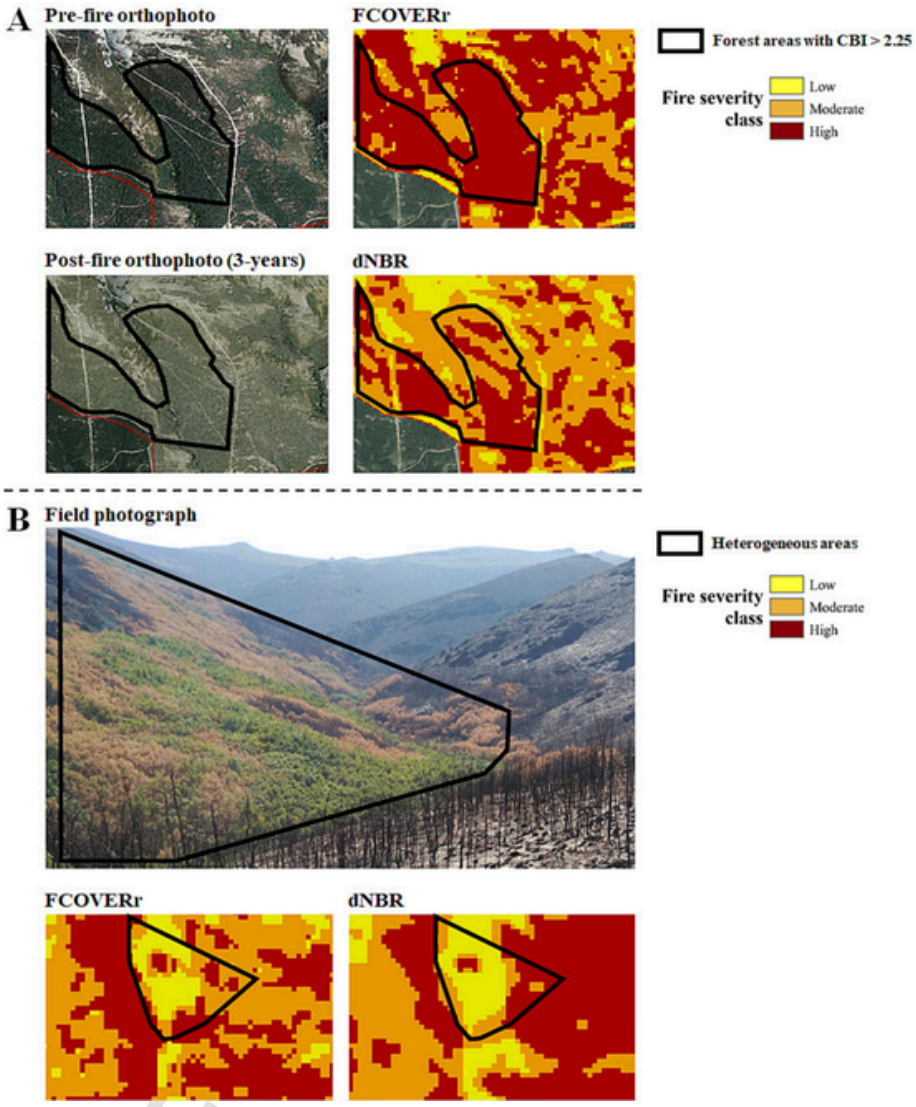

Fig. 8. Detail view of the magnitude of ecological change in a Scots pine forest from pre and post-fire orthophotos (A) and the variation in spatial patchiness of fire severity in a Pyrenean oak forest (B).

nities and sites. This could be explained by the analogous meaning of the variation range in photosynthetic or senesced vegetation estimated through FCOVERr metric to the fire severity definition operationally used in the field (Lentile et al., 2009), together with the lack of physics deemed in the fire severity retrieval using spectral indices, featuring low generalization ability in heterogeneous landscapes comprising multiple plant communities (De Santis and Chuvieco, 2007). In addition, background reflectance of exposed soil and burned legacies can affect the discrimination of fire effects using spectral indices (Meng et al., 2017). Although the shortwave infrared band of traditional broadband spectral indices is often considered to be highly sensitive to ash, char and exposed soil fractions (Miller and Quayle, 2015), it actually is sensitive to a lesser extent than the near infrared band to the vegetation fraction variability (Hudak et al., 2007; Lentile et al., 2009). Therefore, background spectra expansion through reference endmembers of PROSAIL-D reflectance simulations may have been essential to produce more realistic estimates of FCOVER ranges of variation between pre and post-fire scenarios under sparse vegetation canopies (García-Haro et al., 2018).

The complex structure of Mediterranean plant communities does not usually meet the model assumptions for using turbid-medium canopy RTMs as boundary conditions (De Santis et al., 2009), despite being widely used in these types of vegetation for retrieving their biophysical variables with high confidence (Fernández-Guisuraga et al., 2021b). Even so, the version of the selected SAIL canopy RTM, i.e. 4SAIL, can estimate multiple scattering effects inside the canopy and thus describe non-uniform vegetation canopy characteristics (Verhoef et al., 2007; Liang et al., 2015) as compared to previous SAIL model versions. The use of geometric RTMs may be more appropriate and provide better performance in the FCOVER retrieval in Mediterranean plant communities that match such model assumptions (Yebra et al., 2008). De Santis et al. (2009) and De Santis et al. (2010) used the GeoSAIL geometric RTM to simulate spectral reflectance for a range of GeoCBI values which were retrieved from optical reflectance data, achieving a R^2 of 0.91 ± 0.08 in a site with a wide range of measured GeoCBI values in the field, as in our case-study sites, and a R^2 of 0.56 ± 0.18 in two sites with GeoCBI values between 2 and 3. These results slightly improved the performance of the FCOVERr metric for retrieving field-measured fire severity, but at the expense of more complex parameterization for the continuum range of (Geo)CBI values to be used operationally.

The linear relationships between FCOVERr metric and CBI for the Mediterranean plant communities of both case-study sites were also consistent with the results of studies involving reflectance simulations

Table 3
Classification performance of categorized fire severity maps (FCOVERr and dNBR) evaluated through the confusion matrix. We computed the overall accuracy (OA; %), the kappa index, and the user's (UA) and producer's (PA) accuracy (%) of each fire severity class.

		Reference fire severity					
		Sierra de Cabrera			**Navalacruz**		
		Low	Moderate	High	Low	Moderate	High
Classified fire severity **FCOVERr**	Low	57	6	2	65	7	4
	Moderate	4	41	7	8	38	6
	High	0	3	58	2	5	44
	PA (%)	93.44	82.00	86.57	86.67	76.00	81.48
	UA (%)	87.69	78.85	95.08	85.53	73.08	86.28
	OA (%)	**87.64**			**82.12**		
	Kappa index	**0.81**			**0.73**		
		Low	Moderate	High	Low	Moderate	High
Classified fire severity **dNBR**	Low	51	10	6	67	9	5
	Moderate	7	34	12	8	28	9
	High	3	6	49	0	13	40
	PA (%)	83.61	68.00	73.13	89.33	56.00	70.37
	UA (%)	76.12	64.15	84.48	81.71	60.87	74.51
	OA (%)	**75.28**			**74.30**		
	Kappa index	**0.63**			**0.61**		

Table 4
Patch density (PD) and perimeter-area Fractal Dimension Index (p-a FDI) of each fire severity class in Sierra de Cabrera and Navalacruz sites.

		Sierra de Cabrera			**Navalacruz**		
		Low	Moderate	High	Low	Moderate	High
FCOVERr	PD	31.10	35.00	23.20	37.30	37.20	27.60
	p-a FDI	1.51	1.62	1.51	1.54	1.62	1.51
dNBR	PD	14.60	14.50	13.60	13.20	12.80	11.40
	p-a FDI	1.44	1.54	1.40	1.40	1.45	1.42

of fire effects on several multi-strata CBI attributes (De Santis et al., 2009, 2010), which enhanced FCOVERr metric transferability. The generalization power of biophysical variables retrieved from RTM simulations minimized scaling challenges (Fernández-Guisuraga et al., 2021a). In contrast, the type of relationship (i.e. linear or quadratic) between CBI and dNBR/RBR spectral indices was not consistent between sites, which led to transferability issues as expected. These inconsistencies were previously evidenced (Soverel et al., 2010) and may arise from signal saturation of these spectral indices at high fire severities measured in the field (van Wagtendonk et al., 2004; Soverel et al., 2010) and the suboptimal sensitivity of these indices to changes in field-measured fire severity (Roy et al., 2006). This may explain the low transferability performance of dNBR/RBR spectral indices, with errors sometimes exceeding 25% of the CBI range, considered unacceptable to be operationally used as a scalable post-fire assessment product (De Santis and Chuvieco, 2007). It should be noted that the relationship between CBI and RdNBR was linear in both case-study sites, as in some previous studies (e.g. Holden et al., 2009; Stambaugh et al., 2015). However, other studies evidenced non-linear rather than linear correlations (e.g. Miller and Thode, 2007; Parks et al., 2018), or found only marginal improvements in model performance (e.g. Karau et al., 2014; Fernández-García et al., 2018). In this study, the RdNBR performance in the fire severity retrieval scheme was limited (R^2 = 0.50–0.76), and thus its transferability analysis was not considered.

The well-known underestimation of moderate to high fire severities using bi-temporal spectral indices, mainly the dNBR (e.g. Murphy et al., 2008; van Gerrevink and Veraverbeke, 2021), but also the relativized versions (Soverel et al., 2010), were evident not only in the CBI field plots of this study (Figure SM4 of the Supplementary Material), but also through the qualitative assessment of wall-to-wall maps/field observations (Fig. 8), and the quantitative assessment of severity reference data acquired from high spatial resolution aerial/satellite imagery (Table 3). This behavior could be attributed to signal saturation of spectral indices at high fire severity (e.g. van Wagtendonk et al., 2004), a phenomenon that is dependent on vegetation type (Epting et al., 2005; Lentile et al., 2009). Likewise, the patchiness of fire effects, particularly with the occurrence of narrow bands of moderate fire severity levels where a composite of low and severe fire effects combines (Miller et al., 2009), were not properly captured by spectral indices in several areas identified in the field and wall-to-wall estimates (Fig. 8). The low density and shape complexity of patches in the dNBR maps may not be enough to optimally capture the higher landscape heterogeneity and patchiness characterizing burned areas at low and moderate severities as compared to high-severity burned areas (e.g. Harvey et al., 2016; Skowronski). In this sense, the mixed spectral responses of burned canopies at moderate fire severity (i.e. partially scorched) may not be adequately resolved by the limited spectral information used by spectral indices (Rogan and Franklin, 2001; Mallinis et al., 2018). This effect was largely minimized, but still evident, in the FCOVERr estimates probably because of the optical nature of both remote sensing techniques and the potential decoupling of fire severity in the under- and overstory (Miller et al., 2009). The misclassification of fire effects by spectral indices, particularly the confusion between moderate and high fire severity classes in Navalacruz (Table 3), could be a plausible explanation for the differential stand-replacing areas detected in both study sites through wall-to-wall estimates. The higher surface burned at high fire severity detected by the dNBR index in Navalacruz site is mainly registered in the central strip of the wildfire, dominated by Scots pine forests where mixed fire effects in the field tended to concentrate. Indeed, Scots pine is classified in the moderate-severity fire regime and is considered as moderately fire resistant (Granströem, 2001). Therefore, Scots pine forests are characterized by multi-aged stands, being some individuals of the stand considered as fire-avoiders due to increased crown base height (Fernandes et al., 2008), which may contribute to a markedly mixed fire severity pattern. Despite the ecological sense of this argument, this should be further investigated.

We evaluated fire effects by means of the variation of top-of-canopy vegetation fraction in single and multi-layered plant communities, also accounting in the latter case for the lower strata sensed through canopy gaps. This approach may be inappropriate when understory and overstory fire effects are not linked and the overstory layer partly occludes the more severely affected understory layer. Fire severity as assessed in the field would thus be underestimated in these cases, even if they would not be a priority for post-fire rehabilitation (De Santis et al., 2009).

Future research should be focused on validating the FCOVERr metric in a wider variety of Mediterranean plant communities and non-Mediterranean biomes. Although the physical basis of the FCOVERr metric procured an adequate transferability performance between several Mediterranean plant communities and burned landscapes, the application to other Mediterranean communities not considered here, and especially those from other biomes, will require an adequate RTM parameterization to reflect the biophysical settings (i.e. plant traits) of the target vegetation assemblages (Wang et al., 2017). For this purpose, the TRY database (Kattge et al., 2011) exploitation may provide the baseline for a realistic RTM parametrization regarding the leaf and canopy trait variability of the known dominant species in the target communities (Kattenborn et al., 2017). Despite prior plant trait data acquired in the field may provide more realistic RTM simulations by alleviating the ill-posed nature of the models (Yebra and Chuvieco, 2009), highly accurate biophysical estimates can be procured using generic training simulation datasets (e.g. Campos-Taberner et al., 2018). In addition, the broad availability of laboratory and field spectral libraries to expand

RTM simulations with representative background endmember spectra also constitutes the baseline for this approach (Poulter et al., 2023). We must emphasize that we have not included ecosystem responses in the modified CBI protocol because they were negligible in our study sites the month following the fires. Including ecosystem responses into the CBI protocol should be a priority if these are noticeable in the very short-term following fire (De Santis and Chuvieco, 2009) when using our approach in other study sites, or when performing extended fire severity assessments, and the RTM should be parametrized accordingly.

Large-scale fire severity assessments would also benefit from the indirect RTM inversion considered here because of the straightforward and efficient parallel processing framework of the RFR algorithm in cloud-computing platforms (Campos-Taberner et al., 2018). Future research should also compare the performance of the FCOVERr metric retrieved using turbid-medium RTMs with that estimated from geometric models, providing a more comparable scenario than the RTM approaches previously used in the literature.

5. Conclusions

We propose a novel approach with sound ecological and physical sense to assess fire severity through a change detection framework based on the post to pre-fire FCOVER ratio retrieved from passive optical data by inverting the PROSAIL-D RTM. Accurate fire severity retrievals in terms of field-measured CBI were obtained with the FCOVERr metric, and proved to be more transferable than spectral indices in several Mediterranean plant communities because of the generalization power of biophysical variables retrieved from RTM simulations. The FCOVERr metric effectively captured the distribution of moderate to high fire severity areas throughout the heterogeneous patchiness of fire effects, which implies that this product may be a sound alternative for operational use in the identification of priority areas for post-fire management.

Funding

This study was financially supported by the Spanish Ministry of Science and Innovation and NextGenerationEU funds, in the framework of the FIREMAP (TED2021-130925B-I00) project; by the Regional Government of Castilla and León in the framework of the WUIFIRECYL (LE005P20) project; by the British Ecological Society in the framework of the SR22-100154 project, where José Manuel Fernández-Guisuraga is the Principal Investigator; and by national funds from FCT - the Portuguese Foundation for Science and Technology, under the project UIDB/04033/2020. José Manuel Fernández-Guisuraga was supported by a Ramón Areces Foundation postdoctoral fellowship.

Uncited reference

CRediT authorship contribution statement

José Manuel Fernández-Guisuraga : Conceptualization, Methodology, Formal analysis, Investigation, Writing – original draft. **Leonor Calvo :** Conceptualization, Investigation, Writing – review & editing, Supervision, Project administration, Funding acquisition. **Carmen Quintano :** Methodology, Formal analysis, Writing – review & editing. **Alfonso Fernández-Manso :** Methodology, Formal analysis, Writing – review & editing. **Paulo M. Fernandes :** Conceptualization, Formal analysis, Writing – review & editing, Supervision, Project administration, Funding acquisition.

Declaration of Competing Interest

The authors declare that they have no known competing financial interests or personal relationships that could have appeared to influence the work reported in this paper.

Data availability

Data will be made available on request.

Acknowledgements

We thank Dr. Dar Roberts (University of California, Santa Barbara) for providing us with the 2009 AVIRIS image used in this study. We also thank the members of the Editorial Board and the two anonymous reviewers for their comments and suggestions, which have contributed to improve the quality of the manuscript.

Appendix A. Supplementary data

Supplementary data to this article can be found online at https://doi.org/10.1016/j.rse.2023.113542.

References

Archibald, S., Lehmann, C.E.R., Belcher, C.M., Bond, W.J., Bradstock, R.A., Daniau, A.L., Dexter, K.G., Forrestel, E.J., Greve, M., He, T., Higgins, S.I., Hoffmann, W.A., Lamont, B.B., McGlinn, D.J., Moncrieff, G.R., Osborne, C.P., Pausas, J.G., Price, O., Ripley, B.S., Rogers, B.M., Schwilk, D.W., Simon, M.F., Turetsky, M.R., Van der Werf, G.R., Zanne, A.E., 2018. Biological and geophysical feedbacks with fire in the Earth system. Environ. Res. Lett. 13, 033003.

Arneth, A., Harrison, S., Zaehle, S., Tsigaridis, K., Menon, S., Bartlein, P.J., Feichter, J., Korhola, A., Kulmala, M., O'Donnell, D., Schurgers, G., Sorvari, S., Vesala, T., 2010. Terrestrial biogeochemical feedbacks in the climate system. Nat. Geosci. 3, 525–532.

Asner, G., 1998. Biophysical and biochemical sources of variability in canopy reflectance. Remote Sens. Environ. 64, 234–253.

Avitabile, V., Camia, A., 2018. An assessment of forest biomass maps in Europe using harmonized national statistics and inventory plots. For. Ecol. Manag. 409, 489–498.

Barden, L.S., Woods, F.W., 1976. Effects of fire on pine and pine-hardwood forests in the Southern Appalachians. For. Sci. 22, 399–403.

Baret, F., Hagolle, O., Geiger, B., Bicheron, P., Miras, B., Huc, M., Berthelot, B., Niño, F., Weiss, M., Samain, O., Roujean, J.L., Leroy, M., 2007. LAI, fAPAR and fCover CYCLOPES global products derived from VEGETATION: Part 1: Principles of the algorithm. Remote Sens. Environ. 110, 275–286.

Bivand, R., Keitt, T., Rowlingson, B., 2021. rgdal: Bindings for the 'Geospatial' Data Abstraction Library R package version 15-23. https://CRANR-projectorg/package=rgdal.

Breiman, L., 2001. Random forests. Mach. Learn. 45, 5–32.

Botella-Martínez, M.A., Fernández-Manso, A., 2017. Estudio de la severidad post-incendio en la comunidad Valenciana comparando los índices dNBR, RdNBR y RBR a partir de imágenes landsat 8. Revista de Teledetección 49, 33–47.

Campos-Taberner, M., Moreno-Martínez, Á., García-Haro, F.J., Camps-Valls, G., Robinson, N.P., Kattge, J., Running, S.W., 2018. Global estimation of biophysical variables from Google Earth Engine platform. Remote Sens. 10, 1167.

Certini, G., 2005. Effects of fire on properties of forest soils: a review. Oecologia 143, 1–10.

Chuvieco, E., Riaño, D., Danson, F.M., Martin, P., 2006. Use of a radiative transfer model to simulate the postfire spectral response to burn severity. J. Geophys. Res. 111, G04S09.

De Luis, M., González-Hidalgo, J.C., Raventós, J., 2003. Effects of fire and torrential rainfall on erosion in a Mediterranean gorse community. Land Degrad. Dev. 14, 203–213.

De Santis, A., Chuvieco, E., 2007. Burn severity estimation from remotely sensed data: performance of simulation versus empirical models. Remote Sens. Environ. 108, 422–435.

De Santis, A., Chuvieco, E., 2009. GeoCBI: a modified version of the composite burn index for the initial assessment of the short-term burn severity from remotely sensed data. Remote Sens. Environ. 113, 554–562.

De Santis, A., Chuvieco, E., Vaughan, P.J., 2009. Short-term assessment of burn severity using the inversion of PROSPECT and GeoSail models. Remote Sens. Environ. 113, 126–136.

De Santis, A., Asner, G.P., Vaughan, P.J., Knapp, D.E., 2010. Mapping burn severity and burning efficiency in California using simulation models and landsat imagery. Remote Sens. Environ. 114, 1535–1545.

Díaz-Delgado, R., Lloret, F., Pons, X., Terradas, J., 2002. Satellite evidence of decreasing resilience in Mediterranean plant communities after recurrent wildfires. Ecology 83, 2293–2303.

Dörnhöfer, K., Göritz, A., Gege, P., Pflug, B., Oppelt, N., 2016. Water constituents and

water depth retrieval from sentinel-2A—a first evaluation in an oligotrophic lake. Remote Sens. 8, 941.
Edwards, A.C., Russell-Smith, J., Maier, S.W., 2018. A comparison and validation of satellite-derived fire severity mapping techniques in fire prone north Australian savannas: extreme fires and tree stem mortality. Remote Sens. Environ. 206, 287–299.
Epting, J., Verbyla, D., Sorbel, B., 2005. Evaluation of remotely sensed indices for assessing burn severity in interior Alaska using Landsat TM and ETM+. Remote Sens. Environ. 96, 328–339.
Farris, C.A., Margolis, E.Q., Kupfer, J.A., 2008. Spatial characteristics of fire severity in relation to fire growth in a Rocky Mountain subalpine forest. In: Narog, M.G. (tech. coord.). Proceedings of the 2002 Fire Conference: Managing fire and fuels in the remaining wildlands and open spaces of the Southwestern United States. Gen. Tech. Rep. PSW-GTR-189. Albany, CA: U.S. Department of Agriculture, Forest Service, Pacific Southwest Research Station. pp. 175–184.
Féret, J.B., Gitelson, A.A., Noble, S.D., Jacquemoud, S., 2017. PROSPECT-D: towards modeling leaf optical properties through a complete lifecycle. Remote Sens. Environ. 193, 204–215.
Fernandes, P.M., Luz, A., Loureiro, C., 2010. Changes in wildfire severity from maritime pine woodland to contiguous forest types in the mountains of northwestern Portugal. For. Ecol. Manag. 260, 883–892.
Fernandes, P.M., Loureiro, C., Guiomar, N., Pezzatti, G.B., Manso, F.T., Lopes, L., 2014. The dynamics and drivers of fuel and fire in the Portuguese public forest. J. Environ. Manag. 146, 373–382.
Fernandes, P.M., Vega, J.A., Jiménez, E., Rigolot, E., 2008. Fire resistance of European pines. For. Ecol. Manag. 256, 246–255.
Fernández-García, V., Santamarta, M., Fernández-Manso, A., Quintano, C., Marcos, E., Calvo, L., 2018. Burn severity metrics in fire-prone pine ecosystems along a climatic gradient using Landsat imagery. Remote Sens. Environ. 206, 205–217.
Fernández-Guisuraga, J.M., Suárez-Seoane, S., Calvo, L., 2019. Modeling Pinus pinaster forest structure after a large wildfire using remote sensing data at high spatial resolution. For. Ecol. Manag. 446, 257–271.
Fernández-Guisuraga, J.M., Calvo, L., Suárez-Seoane, S., 2020. Comparison of pixel unmixing models in the evaluation of post-fire forest resilience based on temporal series of satellite imagery at moderate and very high spatial resolution. ISPRS J. Photogramm. Remote Sens. 164, 217–228.
Fernández-Guisuraga, J.M., Suárez-Seoane, S., Calvo, L., 2021a. Radiative transfer modeling to measure fire impact and forest engineering resilience at short-term. ISPRS J. Photogramm. Remote Sens. 176, 30–41.
Fernández-Guisuraga, J.M., Verrelst, J., Calvo, L., Suárez-Seoane, S., 2021b. Hybrid inversion of radiative transfer models based on high spatial resolution satellite reflectance data improves fractional vegetation cover retrieval in heterogeneous ecological systems after fire. Remote Sens. Environ. 255, 112304.
Fernández-Guisuraga, J.M., Suárez-Seoane, S., Quintano, C., Fernández-Manso, A., Calvo, L., 2022a. Comparison of physical-based models to measure forest resilience to fire as a function of burn severity. Remote Sens. 14, 5138.
Fernández-Guisuraga, J.M., Suárez-Seoane, S., Calvo, L., 2022b. Radar and multispectral remote sensing data accurately estimate vegetation vertical structure diversity as a fire resilience indicator. Remote Sens. Ecol. Conserv. in press.
Flombaum, P., Sala, O.E., 2009. Cover is a good predictor of aboveground biomass in arid systems. J. Arid Environ. 73, 597–598.
García-Haro, F.J., Campos-Taberner, M., Muñoz-Marí, J., Laparra, V., Camacho, F., Sánchez-Zapero, J., Camps-Valls, G., 2018. Derivation of global vegetation biophysical parameters from EUMETSAT polar system. ISPRS J. Photogramm. Remote Sens. 139, 57–74.
Granströem, A., 2001. Fire management for biodiversity in the European boreal forest. Scand. J. For. Res. 3, 62–69.
Gould, K.S., 2004. Nature's swiss army knife: the diverse protective roles of anthocyanins in leaves. J. Biomed. Biotechnol. 5, 314–320.
Gutman, G., Ignatov, A., 1998. The derivation of the green vegetation fraction from NOAA/AVHRR data for use in numerical weather prediction models. Int. J. Remote Sens. 19, 1533–1543.
Harris, S., Veraverbeke, S., Hook, S., 2011. Evaluating spectral indices for assessing fire severity in chaparral ecosystems (Southern California) using MODIS/ASTER (MASTER) airborne simulator data. Remote Sens. 3, 2403–2419.
Harvey, B.J., Donato, D.C., Turner, M.G., 2016. Drivers and trends in landscape patterns of stand-replacing fire in forests of the US Northern Rocky Mountains (1984–2010). Landsc. Ecol. 31, 2367–2383.
Hauser, L.T., Timmermans, J., van der Windt, N., Sil, Â.F., César de Sá, N., Soudzilovskaia, N.A., van Bodegom, P.M., 2021. Explaining discrepancies between spectral and in-situ plant diversity in multispectral satellite earth observation. Remote Sens. Environ. 265, 112684.
Hesselbarth, M.H.K., Sciaini, M., With, K.A., Wiegand, K., Nowosad, J., 2019. Landscapemetrics: an open-source R tool to calculate landscape metrics. Ecography 42, 1648–1657.
Hijmans, R.J., 2021. raster: Geographic Data Analysis and Modeling R package version 34-10. https://CRANR-projectorg/package=raster.
Holden, Z.A., Morgan, P., Evans, J.S., 2009. A predictive model of burn severity based on 20-year satellite-inferred burn severity data in a large southwestern US wilderness area. For. Ecol. Manag. 258, 2399–2406.
Hood, S.M., Cluck, D.R., Smith, S.L., Ryan, K.C., 2008. Using bark char codes to predict post-fire cambium mortality. Fire Ecol. 4, 57–73.
Hudak, A.T., Morgan, P., Bobbitt, M.J., Smith, A.M.S., Lewis, S.A., Lentile, L.B., Robichaud, P.R., Clark, J.T., McKinley, R.A., 2007. The relationship of multispectral satellite imagery to immediate fire effects. Fire Ecol. 3, 64–90.
Hudak, A.T., Ottmar, R.D., Vihnanek, R.E., Brewer, N.W., Smith, A.M.S., Morgan, P., 2013. The relationship of post-fire white ash cover to surface fuel consumption. Int. J. Wildland Fire 22, 780–785.
Huemmrich, K.F., 2001. The GeoSail model: a simple addition to the SAIL model to describe discontinuous canopy reflectance. Remote Sens. Environ. 75, 423–431.
Jacquemoud, S., Baret, F., 1990. PROSPECT: a model of leaf optical properties spectra. Remote Sens. Environ. 34, 75–91.
Huerta, S., Marcos, E., Fernández-García, V., Calvo, L., 2022. Short-term effects of burn severity on ecosystem multifunctionality in the Northwest Iberian Peninsula. Sci. Total Environ. 844, 157193.
Jia, K., Liang, S., Gu, X., Baret, F., Wei, X., Wang, X., Yao, Y., Yang, L., Li, Y., 2016. Fractional vegetation cover estimation algorithm for Chinese GF-1 wide field view data. Remote Sens. Environ. 177, 184–191.
Jiang, Y., Zhang, Y., Wu, Y., Hu, R., Zhu, J., Tao, J., Zhang, T., 2017. Relationships between aboveground biomass and plant cover at two spatial scales and their determinants in northern Tibetan grasslands. Ecol. Evol. 7, 7954–7964.
Jones, A., Ugalde, O., Scarpa, S., 2020. LUCAS 2015 Topsoil Survey, EUR 30332 EN. Publications Office of the European Union, Luxembourg. https://doi.org/10.2760/616084ISBN 978-92-76-21080-1.
Karau, E.C., Sikkink, P.G., Keane, R.E., Dillon, G.K., 2014. Integrating satellite imagery with simulation modeling to improve burn severity mapping. Environ. Manag. 54, 98–111.
Kasischke, E.S., Turetsky, M.R., Ottmar, R.D., French, N.H.F., Hoy, E.E., Kane, E.S., 2008. Evaluation of the composite burn index for assessing fire severity in Alaskan black spruce forests. Int. J. Wildland Fire 17, 515–526.
Kattenborn, T., Fassnacht, F.E., Pierce, S., Lopatin, J., Grime, J.P., Schmidtlein, S., 2017. Linking plant strategies and plant traits derived by radiative transfer modelling. J. Veg. Sci. 28, 717–727.
Kattge, J., et al., 2011. TRY-a global database of plant traits. Glob. Chang. Biol. 17, 2905–2935.
Keeley, J.E., 2009. Fire intensity, fire severity and burn severity: a brief review and suggested usage. Int. J. Wildland Fire 18, 116–126.
Ketterings, Q.M., Bingham, J.M., 2000. Soil color as an indicator of slash-and-burn severity and soil fertility in Sumatra, Indonesia. Soil Sci. Soc. Am. J. 64, 1826–1833.
Key, C.H., Benson, N., 2005. Landscape assessment: Ground measure of severity, the Composite Burn Index; and remote sensing of severity, the Normalized Burn Ratio. In: FIREMON: Fire Effects Monitoring and Inventory System (D.C. Lutes, R.E. Keane, J.F. Caratti, C.H. Key, N.C. Benson and L.J. Gangi, Eds.), USDA Forest Service, Rocky Mountain Research Station, Gen. Tech. Rep. RMRS-GTR-164, Ogden, UT. CD: LA1–LA51.
Key, C.H., 2006. Ecological and sampling constraints on defining landscape fire severity. Fire Ecol. 2, 34–59.
Kuusk, A., 2001. A two layer canopy reflectance model. J. Quant. Spectrosc. Radiat. Transf. 71, 1–9.
Kuusk, A., Nilson, T., 2000. A directional multispectral forest reflectance model. Remote Sens. Environ. 72, 244–252.
Lentile, L.B., Holden, Z.A., Smith, A.M.S., Falkowski, M.J., Hudak, A.T., Morgan, P., Lewis, S.A., Gessler, P.E., Benson, N.C., 2006. Remote sensing techniques to assess active fire characteristics and post-fire effects. Int. J. Wildland Fire 15, 319–345.
Lentile, L.B., Smith, A.M.S., Hudak, A.T., Morgan, P., Bobbitt, M.J., Lewis, S.A., Robichaud, P.R., 2009. Remote sensing for prediction of 1-year post-fire ecosystem condition. Int. J. Wildland Fire 18, 594–608.
Lewis, S.A., Hudak, A.T., Ottmar, R.D., Robichaud, P.R., Lentile, H.B., Hood, S.M., Cronan, J.B., Morgan, P., 2011. Using hyperspectral imagery to estimate forest floor consumption from wildfire in boreal forests of Alaska, USA. Int. J. Wildland Fire 20, 255–271.
Liang, L., Di, L., Zhang, L., Deng, M., Qin, Z., Zhao, S., Lin, H., 2015. Estimation of crop LAI using hyperspectral vegetation indices and a hybrid inversion method. Remote Sens. Environ. 165, 123–134.
Liaw, A., Wiener, M., 2002. Classification and regression by RandomForest. R News 2, 18–22.
López-García, M.J., Caselles, V., 1991. Mapping burns and natural reforestation using thematic mapper data. Geocarto Int. 1, 31–37.
Mallinis, G., Mitsopoulos, I., Chrysafi, I., 2018. Evaluating and comparing sentinel 2A and Landsat-8 Operational Land Imager (OLI) spectral indices for estimating fire severity in a Mediterranean pine ecosystem of Greece. GISci.Remote Sens. 55, 1–18.
McGarigal, K., Cushman, S.A., Ene, E., 2012. FRAGSTATS v4: Spatial Pattern Analysis Program for Categorical and Continuous Maps. Computer software program produced by the authors at the University of Massachusetts, Amherst. Available at the following web site: http://www.umass.edu/landeco/research/fragstats/fragstats.html.
McKay, M.D., Beckman, R.J., Conover, W.J., 1979. A comparison of three methods for selecting values of input variables in the analysis of output from a computer code. Technometrics 21, 239–245.
Meerdink, S.K., Hook, S.J., Roberts, D.A., Abbott, E.A., 2019. The ECOSTRESS spectral library version 1.0. Remote Sens. Environ. 230, 111196.
Meng, R., Wu, J., Schwager, K.L., Zhao, F., Dennison, P.E., Cook, B.D., Brewster, K., Green, T.M., Serbin, S.P., 2017. Using high spatial resolution satellite imagery to map forest burn severity across spatial scales in a pine barrens ecosystem. Remote Sens. Environ. 191, 95–109.
Meng, R., Wu, J., Zhao, F., Cook, B.D., Hanavan, R.P., Serbin, S.P., 2018. Measuring short-term post-fire forest recovery across a burn severity gradient in a mixed pine-oak forest using multi-sensor remote sensing techniques. Remote Sens. Environ. 210, 282–296.
Migliavacca, M., Dosio, A., Camia, A., Hobourg, R., Houston-Durrant, T., Kaiser, J.W., Khabarov, N., Krasovskii, A.A., Marcolla, B., San Miguel-Ayanz, J., Ward, D.S., Cescatti, A., 2013. Modeling biomass burning and related carbon emissions during the 21st century in Europe. J. Geophys.Res.Biogeosci. 118, 1732–1747.
Miller, J.D., Thode, A.E., 2007. Quantifying burn severity in a heterogeneous landscape

with a relative version of the delta normalized burn ratio (dNBR). Remote Sens. Environ. 109, 66–80.
Miller, J.D., Knapp, E.C., Key, C.H., Skinner, C.N., Isbell, C.J., Creasy, R.M., Sherlock, J.W., 2009. Calibration and validation of the relative differenced normalized burn ratio (RdNBR) to three measures of fire severity in the Sierra Nevada and Klamath Mountains, California, USA. Remote Sens. Environ. 113, 645–656.
Miller, J.D., Quayle, B., 2015. Calibration and validation of immediate post-fire satellite-derived data to three severity metrics. Fire Ecol. 11, 12–30.
Mitri, G.H., Gitas, I.Z., 2008. Mapping the severity of fire using object-based classification of IKONOS imagery. Int. J. Wildland Fire 17, 431–442.
Morgan, P., Hudak, A.T., Robichaud, P.R., Ryan, K.C., 2005. Assessing the causes, consequences and spatial variability of burn severity: a rapid response proposal. Joint Fire Science Project 03-2-1-02. Moscow, ID. University of Idaho, Forest Resources Department. 21 p.
Morgan, P., Keane, R.E., Dillon, G.K., Jain, T.B., Hudak, A.T., Karau, E.C., Sikkink, P.G., Holden, Z.A., Strand, E.K., 2014. Challenges of assessing fire and burn severity using field measures, remote sensing and modelling. Int. J. Wildland Fire 23, 1045–1060.
Murphy, K.A., Reynolds, K.H., Koltun, J.M., 2008. Evaluating the ability of the differenced normalized burn ratio (dNBR) to predict ecologically significant burn severity in alaskan boreal forests. Int. J. Wildland Fire 17, 490–499.
Nachtergaele, F., van Velthuizen, H., Verelst, L., Batjes, N., Dijkshoorn, K., van Engelen, E., Fischer, G., Jones, A., Montanarela, L., Petri, M., Prieler, S., Shi, X., Teixeira, E., Wiberg, D., 2010. The harmonized world soil database. In: Proceedings of the 19th World Congress of Soil Science, Soil Solutions for a Changing World. Brisbane, Australia, 1-6 August 2010. pp. 34–37.
Ninyerola, M., Pons, X., Roure, J.M., 2005. Atlas Climático Digital de la Península Ibérica. Metodología y aplicaciones en bioclimatología y geobotánica. Universidad Autónoma de Barcelona. dataset.
Nogueira, J.M.P., Ruffault, J., Chuvieco, E., Mouillot, F., 2017. Can we go beyond burned area in the assessment of global remote sensing products with fire patch Metrics? Remote Sens. 9, 7.
Nolè, A., Rita, A., Spatola, M.F., Borghetti, M., 2022. Biogeographic variability in wildfire severity and post-fire vegetation recovery across the European forests via remote sensing-derived spectral metrics. Sci. Total Environ. 823, 153807.
Norton, J., Glenn, N., Germino, M., Weber, K., Seefeldt, S., 2009. Relative suitability of indices derived from Landsat ETM + and SPOT 5 for detecting fire severity in sagebrush steppe. Int. J. Appl. Earth Obs. Geoinf. 11, 360–367.
Parks, S.A., Dillon, G.K., Miller, C., 2014. A new metric for quantifying burn severity: the relativized burn ratio. Remote Sens. 6, 1827–1844.
Parks, S.A., Holsinger, L.M., Voss, M.A., Loehman, R.A., Robinson, N.P., 2018. Mean composite fire severity metrics computed with Google Earth Engine offer improved accuracy and expanded mapping potential. Remote Sens. 10, 1–15.
Pérez, B., Moreno, J.M., 1998. Methods for quantifying fire severity in shrubland-fires. Plant Ecol. 139, 91–101.
Pérez-Valera, E., Verdú, M., Navarro-Cano, J.A., Goberna, M., 2020. Soil microbiome drives the recovery of ecosystem functions after fire. Soil Biol. Biochem. 149, 107948.
Picotte, J.J., Bhattarai, K., Howard, D., Lecker, J., Epting, J., Quayle, B., Benson, N., Nelson, K., 2020. Changes to the monitoring trends in burn severity program mapping production procedures and data products. Fire Ecol. 16, 16.
Poulter, B., et al., 2023. Simulating global dynamic surface reflectances for imaging spectroscopy spaceborne missions: LPJ-PROSAIL. J. Geophys. Res.Biogeosci. 128, e2022JG006935. https://doi.org/10.1029/2022JG006935.
Probst, P., Boulesteix, A.L., 2018. To tune or not to tune the number of trees in Random Forest. J. Mach. Learn. Res. 18, 1–18.
Quintano, C., Fernández-Manso, A., Roberts, D.A., 2013. Multiple endmember spectral mixture analysis (MESMA) to map burn severity levels from Landsat images in Mediterranean countries. Remote Sens. Environ. 136, 76–88.
Quintano, C., Fernández-Manso, A., Roberts, D.A., 2020. Enhanced burn severity estimation using fine resolution ET and MESMA fraction images with machine learning algorithm. Remote Sens. Environ. 244, 111815.
R Core Team, 2021. R: A Language and Environment for Statistical Computing. R Foundation for Statistical Computing, Vienna, Austria. https://www.R-project.org/.
Richter, R., Schläpfer, D., 2018. Atmospheric/Topographic Correction for Satellite Imagery; DLR Report DLR-IB 565-01/2018; ReSe Applications Schläpfer, Wessling, Germany.
Roberts, D.A., Gardner, M., Church, R., Ustin, S., Scheer, G., Green, R.O., 1998. Mapping chaparral in the Santa Monica Mountains using multiple endmember spectral mixture models. Remote Sens. Environ. 65, 267–279.
Roberts, D.A., Quattrochi, D.A., Hulley, G.C., Hook, S.J., Green, R.O., 2012. Synergies between VSWIR and TIR data for the urban environment: an evaluation of the potential for the hyperspectral infrared imager (HyspIRI) decadal survey mission. Remote Sens. Environ. 117, 83–101.
Rodríguez-Alleres, M., Varela, M.E., Benito, E., 2012. Natural severity of water repellency in pine forest soils from NW Spain and influence of wildfire severity on its persistence. Geoderma 191, 125–131.
Rogan, J., Franklin, J., 2001. Mapping wildfire burn severity in southern California forests and shrublands using enhanced thematic mapper imagery. Geocarto Int. 4, 89–99.
Roy, D.P., Boschetti, L., Trigg, S.N., 2006. Remote sensing of fire severity: assessing the performance of the normalized burn ratio. IEEE Geosci. Remote Sens. Lett. 3, 112–116.
Ryan, K.C., Noste, N.V., 1983. Evaluating prescribed fires. In: Lotan, J.E., Kilgore, B.M., Fischer, W.C., Mutch, R.W. (Eds.), Symposium and Workshop on Wilderness Fire. Missoula, MT: USDA Forest Service, Intermountain Forest and Range Experiment Station, Ogden, UT, General Technical Report, INT-182. pp. 230–238.
Sáenz de Miera, L.E., Pinto, R., Gutierrez-Gonzalez, J.J., Calvo, L., Ansola, G., 2020. Wildfire effects on diversity and composition in soil bacterial communities. Sci. Total Environ. 726, 138636.
San-Miguel-Ayanz, J., Durrant, T., Boca, R., Maianti, P., Liberta, G., Artes Vivancos, T., Jacome Felix Oom, D., Branco, A., De Rigo, D., Ferrari, D., Pfeiffer, H., Grecchi, R., Nuijten, D., Onida, M., Loffler, P., 2021. Forest Fires in Europe, Middle East and North Africa 2020, EUR 30862 EN. Publications Office of the European Union, Luxembourg.
Santín, C., Doerr, S.H., 2016. Fire effects on soils: the human dimension. Philos. Trans. R. Soc. B 371, 20150171.
Schepers, L., Haest, B., Veraverbeke, S., Spanhove, T., Vanden Borre, J., Goossens, R., 2014. Burned area detection and burn severity assessment of a heathland fire in Belgium using airborne imaging spectroscopy (APEX). Remote Sens. 6, 1803–1826.
Skowronski, N.S., Gallagher, M.R., Warner, T.A., 2020. Decomposing the interactions between fire severity and canopy fuel structure using multi-temporal, active, and passive remote sensing approaches. Fire 3, 7.
Soverel, N.O., Perrakis, D.D.B., Coops, N.C., 2010. Estimating burn severity from landsat dNBR and RdNBR indices across western Canada. Remote Sens. Environ. 114, 1896–1909.
Stambaugh, M.C., Hammer, L.D., Godfrey, R., 2015. Performance of burn-severity metrics and classification in oak woodlands and grasslands. Remote Sens. 7, 10501–10522.
Tanase, M.A., Kennedy, R., Aponte, C., 2015. Radar burn ratio for fire severity estimation at canopy level: an example for temperate forests. Remote Sens. Environ. 170, 14–31.
Tessler, N., Sapir, Y., Wittenberg, L., Greenbaum, N., 2016. Recovery of Mediterranean vegetation after recurrent Forest fires: insight from the 2010 Forest fire on Mount Carmel, Israel. Land Degrad. Dev. 27, 1424–1431.
Thompson, J.R., Spies, T.A., 2009. Vegetation and weather explain variation in crown damage within a large mixed-severity wildfire. For. Ecol. Manag. 258, 1684–1694.
Úbeda, X., Outeiro, L.R., Sala, M., 2006. Vegetation regrowth after a differential intensity forest fire in a Mediterranean environment, Northeast Spain. Land Degrad. Dev. 17, 429–440.
van Gerrevink, M.J., Veraverbeke, S., 2021. Evaluating the near and mid infrared bi-spectral space for assessing fire severity and comparison with the differenced normalized burn ratio. Remote Sens. 13, 695.
van Wagtendonk, J.W., Root, R.R., Key, C.H., 2004. Comparison of AVIRIS and landsat ETM+ detection capabilities for burn severity. Remote Sens. Environ. 92, 397–408.
Vega, J.A., Fontúrbel, T., Merino, A., Fernández, C., Ferreiro, A., Jiménez, E., 2013. Testing the ability of visual indicators of soil burn severity to reflect changes in soil chemical and microbial properties in pine forests and shrubland. Plant Soil 369, 73–91.
Veraverbeke, S., Lhermitte, S., Verstraeten, W.W., Goossens, R., 2010. The temporal dimension of differenced normalized burn ratio (dNBR) fire/burn severity studies: the case of the large 2007 Peloponnese wildfires in Greece. Remote Sens. Environ. 114, 2548–2563.
Veraverbeke, S., Gitas, I., Katagis, T., Polychronaki, A., Somers, B., Goossens, R., 2012. Assessing post-fire vegetation recovery using red–near infrared vegetation indices: accounting for background and vegetation variability. ISPRS J. Photogramm. Remote Sens. 68, 28–39.
Verhoef, W., Xiao, Q., Jia, L., Su, Z., 2007. Unified optical-thermal four-stream radiative transfer theory for homogeneous vegetation canopies. IEEE Trans. Geosci. Remote Sens. 45, 1808–1822.
Verrelst, J., Romijn, E., Kooistra, L., 2012. Mapping vegetation structure in a heterogeneous river floodplain ecosystem using pointable CHRIS/PROBA data. Remote Sens. 4, 2866–2889.
Verrelst, J., Rivera, J.P., Veroustraete, F., Muñoz-Marí, J., Clevers, J.G.P.W., Camps-Valls, G., Moreno, J., 2015. Experimental Sentinel-2 LAI estimation using parametric, non-parametric and physical retrieval methods – a comparison. ISPRS J. Photogramm. Remote Sens. 108, 260–272.
Verrelst, J., Rivera, J.P., Gitelson, A., Delegido, J., Moreno, J., Camps-Valls, G., 2016. Spectral band selection for vegetation properties retrieval using Gaussian processes regression. Int. J. Appl. Earth Obs. Geoinf. 52, 554–567.
Verstraete, M.M., Pinty, B., 1996. Designing optimal spectral indices for remote sensing applications. IEEE Trans. Geosci. Remote Sens. 34, 1254–1265.
Wang, B., Jia, K., Liang, S., Xie, X., Wei, X., Zhao, X., Yao, Y., Zhang, X., 2018. Assessment of Sentinel-2 MSI spectral band reflectances for estimating fractional vegetation cover. Remote Sens. 10, 1927.
Ward, D.S., Kloster, S., Mahowald, N.M., Rogers, B.M., Randerson, J.T., Hess, P.G., 2012. The changing radiative forcing of fires: global model estimates for past, present and future. Atmos. Chem. Phys. 12, 10857–10886.
Wang, X., Jia, K., Liang, S., Li, Q., Wei, X., Yao, Y., Zhang, X., Tu, Y., 2017. Estimating fractional vegetation cover from Landsat-7 ETM+ reflectance data based on a coupled radiative transfer and crop growth model. IEEE Trans. Geosci. Remote Sens. 55, 5539–5546.
Wang, J., Lopez-Lozano, R., Weiss, M., Buis, S., Li, W., Liu, S., Baret, F., Zhang, J., 2022. Crop specific inversion of PROSAIL to retrieve green area index (GAI) from several decametric satellites using a bayesian framework. Remote Sens. Environ. 278, 113085.
Welch, K.R., Safford, H.D., Young, T.P., 2016. Predicting conifer establishment post wildfire in mixed conifer forests of the North American Mediterranean-climate zone. Ecosphere 7, e01609.
Yebra, M., Chuvieco, E., Riaño, D., 2008. Estimation of live fuel moisture content from MODIS images for fire risk assessment. Agric. For. Meteorol. 148, 523–536.
Yebra, M., Chuvieco, E., 2009. Linking ecological information and radiative transfer models to estimate fuel moisture content in the Mediterranean region of Spain: solving the ill-posed inverse problem. Remote Sens. Environ. 113, 2403–2411.
Yin, C., He, B., Yebra, M., Quan, X., Edwards, A.C., Liu, X., Liao, Z., 2020a. Improving burn severity retrieval by integrating tree canopy cover into radiative transfer model simulation. Remote Sens. Environ. 236, 111454.
Yin, C., He, B., Quan, X., Yebra, M., Lai, G., 2020b. Remote sensing of burn severity using

coupled radiative transfer model: a case study on Chinese Qinyuan Pine fires. Remote Sens. 12, 3590.